High Performing Visible Light Active Ag_3PO_4/TiO_2 Catalyst Anchored on Alumina Beads for Phenol Degradation

By

LAEEQ MAZHAR

NUST201463481MSCEE65214F

A thesis submitted in partial fulfilment of the requirements for the degree of

Master of Science

In

Environmental Science

Institute of Environmental Sciences and Engineering (IESE)

School of Civil and Environmental Engineering (SCEE)

National University of Sciences and Technology (NUST)

Islamabad, Pakistan

2017

It is certified that the contents and forms of the thesis entitled

High Performing Visible Light Active Ag_3PO_4/TiO_2 Catalyst Anchored on Alumina Beads for Phenol Degradation

Submitted by

LAEEQ MAZHAR

Has been found satisfactory for the requirements of the degree of
Master of Science in Environmental Science

Supervisor: _____
Dr. Zeeshan Ali Khan
Assistant Professor
IESE, SCEE, NUST

Member: _____
Dr. Anwar Baig
Professor
IESE, SCEE, NUST

Member:_____
Engr. Arsalan Khalid
Lecturer
IESE, SCEE, NUST

DEDICATED TO…

MY BELOVED PARENTS, BROTHER AND RESPECTED TEACHERS

WITHOUT THEIR SUPPORT ALL THIS WOULD NOT HAVE BEEN POSSIBLE

ACKNOWLEDGEMENTS

This dissertation would not have been possible without the guidance and the help of several individuals who in one way or another contributed and extended their valuable assistance in planning, executing and finally, presentation, of this study.

First and foremost, I would like to express my sincere gratitude to my thesis supervisor Assistant Prof. **Dr. Zeeshan Ali Khan** (IESE) for his continuous support throughout my stay at IESE, for his patience, motivation, enthusiasm, and immense knowledge. His guidance helped me through my research and writing of this thesis. I could not have imagined having a better advisor and mentor for my MS studies.

Many thanks also go to **Dr. Anwar Baig** (IESE) and **Engr. Arsalan Khalid** (IESE) for their guidance and support.

I am also very thankful to the **Dr. Ishtiaq A. Qazi** for his unfailing moral support and guidance.

I am grateful to the staff of the Waste Water and Chemistry Lab, for the technical assistance. Last but not least, I would like to express my gratitude to all my friends, for their support during this arduous academic odyssey.

Laeeq Mazhar

Table of Contents

Chapter 1 1

Introduction 1

1.1 Background 1

1.2 TiO_2 Photocatalyst 1

1.3 Silver Phosphate (Ag_3PO_4) Photocatalyst 2

1.4 Immobilization of Photocatalyst 3

1.5 Target Pollutant (Phenol) 3

1.6 Objectives 4

1.7 Significance of Work 4

Chapter 2 5

Literature Review 5

2.1 Background 5

2.2 Ag doped TiO_2 6

2.3 Visible Light Responsive Silver Phosphate (Ag_3PO_4) Photocatalyst 7

2.4 Photo-corrosion Phenomenon 7

2.5 Ag_3PO_4/TiO_2 Composite 8

2.6 Self-Corrosion Phenomenon 9

2.7 Immobilization of Nanoparticles 10

2.7.1 Drawbacks of Suspended Nanoparticles 10

2.7.2 Advantages of Immobilized Nanoparticles 11

2.7.3 Drawbacks of Immobilized Nanoparticles 11

2.8 Immobilization Substrates 12

2.8.1 Characteristics of Good Substrate 12

2.8.2 Alumina Beads as Support Substrate 13

2.9 Methods for Immobilization 14

2.10 Phenol (Target Pollutant) 14

2.10.1 Industrial Uses of Phenol 15

2.10.2 Sources of Phenol 15

2.10.3 Environmental Effects of Phenol 16

2.10.4 Permissible Limits of Phenol 16

Chapter 3 17

Materials & Methods 17

3.1 Materials 17
3.2 Synthesis of Titania (TiO_2) Nanoparticles 17
3.3 Synthesis of Ag_3PO_4/TiO_2 Nanoparticles 18
3.4 Immobilization of Nanoparticles onto Alumina (Al_2O_3) Beads 19
3.5 Characterization 20
3.6 Experimental Setup 21
3.7 Adsorption Isotherm Model 22
3.8 Photo-degradation Kinetic Study 23
Chapter 4 25
Results and Discussion 25
4.1 Characterization 25
4.2 Catalyst Performance Evaluation 27
4.2.1 Effect of pH 28
4.2.2 Effect of catalyst dose 29
4.2.3 Effect of Initial Concentration 30
4.2.4 Photocatalysis under UV and Visible light 31
4.3 Adsorption Isotherm Models 33
4.4 Photo-degradation Kinetic Study 36
Chapter 5 42
Conclusions & Recommendations 42
5.1 Conclusions 42
5.2 Recommendations 43
Chapter 6 44
References 44

LIST OF ABBREVIATIONS

EDS	Energy Dispersive Spectroscopy
IESE	Institute of Environmental Sciences and Engineering
SEM	Scanning Electron Microscopy
TiO_2	Titanium Dioxide
Ag- TiO_2	Silver doped Titanium Dioxide
Ag_3PO_4	Silver Phosphate
UV	Ultra Violet
Vis	Visible
XRD	X - Ray Diffraction
λ	Wavelength
US EPA	United States Environmental Protection Agency
NEQS	National Environmental Quality Standards

LIST OF TABLES

Chapter 4

Table 4.1: BET Characteristic Data of TiO_2, Ag-TiO_2 and Ag_3PO_4/TiO_2……**27**

Table 4.2: Adsorption Isotherm model parameters using non-linear regression analysis…….**35**

Table 4.3: Photo-degradation Kinetic Model Parameters (under UV Light)……**40**

Table 4.4: Photo-degradation Kinetic Model Parameters (under Visible Light)……..**41**

LIST OF FIGURES

Chapter 2

Fig. 2.1: Alumina Beads as Immobilization Substrate……..**13**

Fig. 2.2: Phenol (C_6H_5OH)……...**15**

Chapter 3

Fig 1.1: Synthesis of Titania (TiO_2) Nanoparticles…….**18**

Fig 3.2: Synthesis of Ag_3PO_4/TiO_2 Nanoparticles……**19**

Fig3.3: Immobilization of Nanoparticles onto Alumina (Al_2O_3) Beads……...**20**

Fig 3.4: Schematic Diagram of Photocatalytic Reactor……**21**

Chapter 4

Fig. 4.1: XRD pattern of TiO_2, Ag-TiO_2 and Ag_3PO_4/TiO_2 composites ……**25**

Fig. 4.2: SEM Images of (a) Un-coated bead, (b) TiO_2 coated bead, (c) Ag-TiO_2 coated bead, (d) Ag_3PO_4/TiO_2 coated bead……...**26**

Fig. 4.3: EDS Images of (e) Un-coated bead, (f) TiO_2 coated bead, (g) Ag-TiO_2 coated bead, (h) Ag_3PO_4/TiO_2 coated bead……...**27**

Fig. 4.4: Effect of pH on degradation of phenol (initial concentration: 25 ppm, catalyst dose: 30 g/150 ml, contact time: 210 min and temperature: 25 °C)……**29**

Fig. 4.5: Effect of Catalyst Dose on degradation of phenol (pH: 4, initial concentration: 25 ppm, contact time: 210 min and temperature: 25 °C)……**30**

Fig. 4.6: Effect of Initial Concentration degradation of phenol (pH: 4, catalyst dose: 90 g/150 ml, contact time: 210 min and temperature: 25 °C)……...**31**

Fig. 4.7: Photocatalysis of Phenol under (a) UV light (b) Visible Light (pH: 4, initial concentration: 25 ppm, catalyst dose: 90 g/150 ml, contact time: 210 min and temperature: 25 °C)……**33**

Fig. 4.8: Isotherm Model*s* for (a) TiO_2, (b) Ag-TiO_2 and (c) Ag_3PO_4/TiO_2……**35**

Fig. 4.9: Photo-degradation Kinetic Models of (a) TiO_2/UV (b) Ag-TiO_2/UV (c) Ag_3PO_4/TiO_2/UV……**38**

Fig 4.10: Photo-degradation Kinetic Models of (a) TiO_2/Vis (b) Ag-TiO_2/Vis (c) Ag_3PO_4-TiO_2/Vis……...**39**

Abstract

The study explores the development of visible light active photocatalyst for degradation of organic pollutant such as Phenol. Three different photocatalysts (TiO_2, Ag-TiO_2 and Ag_3PO_4/TiO_2) were investigated. Sol gel method was used for the synthesis of TiO_2 and Ag-TiO_2 and in-situ precipitation method for the synthesis of Ag_3PO_4/TiO_2 nanoparticles. The prepared catalysts were immobilized on porous alumina (Al_2O_3) beads and their comparative performance was evaluated under both UV and visible irradiance for phenol mineralization. The surface area, surface morphology, composition and crystal structure of photocatalysts were characterized using Brunauer–Emmett–Teller (BET), scanning electron microscopy (SEM), energy dispersive spectroscopy (EDS) and X-ray diffraction (XRD), respectively. The effects of phenol solution pH, catalyst dose, and initial phenol concentration for phenol degradation were investigated and found to be influential. Langmuir, Freundlich, and Redlich-Peterson (R-P) isotherms models were used to describe adsorption mechanism and Freundlich and R-P model were found to best fit the adsorption data with lowest chi-squared (χ^2) value. Langmuir-Hinshelwood kinetic model best represented the photo-degradation of phenol under both UV and visible light as compared to 1^{st} order and 2^{nd} order kinetic models. The photocatalytic rate constant (K_{L-H}) was significantly greater than the adsorption rate constant (K_{ads}) showing that photocatlysis is the rate determining step.

Keywords: Photocatalysis; visible Light; Silver Phosphate; Titania; Phenol Degradation;

Chapter 1

INTRODUCTION

1.1. Background

TiO_2 has been extensively used as photocatalyst for its low cost, chemical stability, and non-toxic characteristics. Basically, TiO_2 is a favorable photo-oxidation catalyst due to strong oxidizing capability of photo-induced holes, and more commonly, other photocatlysts exhibit less efficiency than TiO_2 under UV irradiation (Zhao et al., 2014). But, TiO_2 has a large band gap of 3.2 eV, which requires UV light for its excitation. We also know that spectrum of sun consists of only 4% UV region whereas 46% visible region (Chen, Dai, & Wang, 2015).

1.2. TiO_2 as Photocatalyst

Titanium dioxide for more than 3 decades has been exploited as heterogeneous photocatalyst after Akira Fujishima and Honda first reported its photocatalytic characteristic for photo-induced decomposition of water. Following properties of TiO_2 made it an efficient photocatalyst: (a) high stability, (b) economically feasible, (c) non-toxic for both the environment and humans, (d) can be immobilized on various substrates, (e) complete degradation of pollutants, (f) high efficiency, (g) strong oxidant, (h) non-photo corrosive, (i) chemically stable. TiO_2 photocatalysis is applicable in following various areas such as: self-cleaning devices and photo-induced coating, self-sterilization, air purification, hydrogen fuel production and wastewater treatment. Use of TiO_2 photocatalyst for hydrogen fuel production has gained a lot of interest in recent years because it is related to the generation of renewable energy without any harmful and GHG emission (Singh, Mahalingam, & Singh, 2013).

1.3. Silver Phosphate (Ag_3PO_4) Photocatalyst

Now a days the research targets on advancement in modification of photocatalysts capable of exploiting the visible region which occupies the bigger share (~46%) of sunlight and Ag_3PO_4 (band gap: 2.85 eV) emerged as one of the most effective catalyst in terms of visible light consumption for mineralization of organic pollutants and environmental remediation (Rashid & Barakat, 2014). O_2 generation from water decomposition as well as organic pollutant mineralization using visible light irradiation assisted by Ag_3PO_4 photocatalyst reveals very high photo-oxidative abilities. More importantly, it can gain a quantum efficiency of almost 90% at the wavelength of 420 nm in water splitting using $AgNO_3$ scavenger, showing its extremely high efficiency than the other reported semiconductors, such as, $BiVO_4$ or N-doped TiO_2 (almost 20%). But Ag_3PO_4 application has one most serious disadvantage of undesirable and uninhibited photo-corrosion, which is a major obstacle. This is because Ag_3PO_4 is slight soluble (0.02 g L^{-1}) in solution and its own properties of energy-band structure. The higher conduction band (CB) energy of Ag_3PO_4 (0.45 eV), than the reduced potential of H_2O/H_2, resulting in the uptake of photo-induced electrons by H_2O unmanageable, unless the solution contain no scavengers. Thus, the Ag leached from the crystal lattice of Ag_3PO_4 uptake the electrons, then resulting in the accumulation of Ag^0 on the surface of crystal. This phenomenon results in decreased photocatalytic activity of Ag_3PO_4, because of the reduced light absorption capacity of catalyst and also destruction of its structure. That is why, it is still an active field of research to devise a facile and efficient method for increasing the stability of Ag_3PO_4 as well as maintaining or further enhancing its efficiency without the sacrificial reagents (Chen, Dai, & Wang, 2015).

1.4. Immobilization of Photocatalyst

More often, TiO_2 has been exploited in the form of suspension or slurry, which ends up with numerous problems such as: (i) recovery of catalyst from slurry is difficult, (ii) aggregation of suspended catalyst, (iii) suspension halt the flow of continuous systems, and (iv) because of the high absorption and scattering by TiO_2 particles, light penetration is limited (Sheidaei & Behnajady, 2015). Filtration, coagulation, flocculation or centrifugations are the different schemes for recovery of the catalyst from slurry, which eventually increases the time and cost of post-treatment. To overcome these limitations numerous kinds of immobilization techniques have been developed to anchor the photocatalyst powder (Koohestani, Sadrnezhaad, & Kheilnejad, 2016). Anchoring the photocatalysts on solid substrate will minimize the time and cost of post-treatment and allow the repetitive and extended reuse of catalyst (Saran, Kamalraj, Arunkumar, & Devipriya, 2016).

1.5. Target Pollutant (Phenol)

Organic compounds comprising a phenolic group is an important family of pollutants anthropogenically produced by several chemical industries. They pose the danger of high stability, toxicity and often causes cancer resulting in severe damage to aquatic ecosystem and human life (Vargová et al., 2011). Phenols have been constantly introduced into the water bodies via numerous human induced inputs. Recycling of wastewater still have the major burden of toxic organic pollutants being present in water bodies (Ahmed, Rasul, Martens, Brown, & Hashib, 2011). Phenol compounds have wide applications in industrial and domestic sector resulting in increased contamination of water bodies. The wastewaters of following industries such as: paint, tanneries, textile plants, oil refineries, pharmaceutical, food, and coal processing industries

contains phenol and its compounds. They remain the environment for longer periods because of their constancy and bio-accumulation. High noxiousness and carcinogenicity of phenol and its compounds can result in significant harmful effects on both the aquatic ecosystems and the human health. Phenol has been categorized as priority pollutant by US Environmental Protection Agency because of its high toxicity, carcinogenicity, and persistence (Shet & Shetty K, 2015).

1.6. Objectives

The objectives of this research were:

- Synthesis of TiO_2, Ag doped TiO_2 and Ag_3PO_4/TiO_2 nanoparticles
- Immobilization of nanoparticles on Alumina (Al_2O_3) beads
- Fabrication of a horizontal flat-bed photo-reactor
- Degradation of synthetic phenol solution

1.7. Significance of Work

Synthesis and immobilization of new composite Ag_3PO_4/TiO_2 enables photocatalysis to be done under visible light achieving maximum efficiency. The catalyst being visible light responsive can be exploited using solar light directly or indirectly (using solar panels) making the overall process energy efficient. The immobilization also offers the maximum utilization of catalyst with minimum loss.

Chapter 2

Literature Review

2.1. Background

The photo-induced breakdown of water molecules on TiO_2 electrodes was first reported by Akira Fujishima and Kenichi Honda in 1972. Subsequently the heterogeneous photocatalysis by using titanium dioxide has been considered as a dynamic area of research in the recent years. TiO_2 has been widely used due to the presence of following properties: (i) highly stable, (ii) strong oxidizing nature, (iii) efficient photocatalyst, (iv) non-toxic, (v) cost effective, (vi) complete breakdown of organic contaminants, (vii) economical, (viii) lower band gap, (ix) can be supported on numerous substrates and (x) stable against the photo corrosion.

Even though the TiO_2 photocatalyst has been considered as a best photocatalyst, but it has the following major limitations:

- It can be activated only under the UV irradiations.
- Recombination of photo-induced electron hole pairs which eventually leads to the overall reduction in quantum efficiency.

Extensive research work has been carried out for TiO_2 modification in order to make it more effective under freely available visible light for its large scale commercial applications. Various approaches illustrated in TiO_2 modification are doping, coupling, dye sensitization, capping and surface modification by using noble metals (Singh et al., 2014).

From the last few eras, the photocatalytic degradation of phenol from wastewater is a remarkable alternative and an area of great interest for many researchers. Numerous materials like TiO_2, ZnO, CdS, MgO, ZrO_2, MoS, WO_3, Fe_2O_3 and their combinations have been widely used for the photocatalytic degradation of organic contaminants. Heterogeneous photocatalytic degradation of phenol by using TiO_2 under UV irradiation has considered as an effective process. The recombination of electron-hole pair is considered as a limitation in the use of TiO_2 because it leads to the lower rate of photocatalytic degradation.

Doped TiO_2 results in the reduction of electron-hole recombination which ultimately enhance the catalytic efficiency in terms of photocatalytic degradation of dye molecules, organic contaminants and hexavalent chromium from waste water (Shet & Shetty K, 2015).

2.2. Ag doped TiO_2

Ag a noble metal is one of the best metal for doping due to its easy processing in industrial applications, low cost as well as the best disinfectant agent that can be used in the treatment/purification of contaminated air and water. Actually the electrons generated on the surface of TiO_2 may quickly make their way to the silver particles, which results in the production of more hydroxyl radicals by reducing electron-hole recombination (Altın & Sökmen, 2014).

The TiO_2 particles with efficient photocatalytic activity for photo-oxidation of organic pollutants under visible light can be acquired only when its band gap energy is smaller than 3.2 eV. The absorption band of TiO_2 particles can be converted from UV region to visible by doping the transition metals on the lattice of TiO_2. Ag among the all

transition metals has received considerable attention as its introduction can remarkably extend the absorption of visible light (Rabbani, Bathaee, Rahimi, & Maleki, 2016).

2.3. Visible Light Responsive Silver Phosphate (Ag_3PO_4) Photocatalyst

Ye et al., has reported a new semiconductor, Ag_3PO_4 in the recent years as an innovation in the field of visible light driven photocatalytic degradation. As it revealed tremendously high photo-oxidation abilities for the production of O_2 from water and the degradation of organic pollutants under visible light (Ma et al., 2014).

By using the available solar radiations, photocatalysis has gained much attention in the prospect of research in the recent years which can be considered as a better option in solving the problems related to energy crisis as well as the environmental contaminants. Among all the photocatalytic materials, Ag_3PO_4 was stated as an excellent photocatalyst under visible light due to its high photo-oxidation capability for O_2 production from water and the photocatalytic degradation of organic contaminats under visible irradiations (Wan et al., 2015).

Recently, the use of Ag_3PO_4 has been proved as a best responsive photocatalyst for visible light, which reveals high quantum yield (~ 90%) at the wavelength less than 480 nm for the production of O_2, and also shows greater photocatalytic degradation rate for organic pollutants (T. Liu et al., 2015).

2.4. Photo-corrosion Phenomenon

Stability of Ag_3PO_4 photocatalyst is the chief limitation for its practical use as a highly efficient and recyclable photocatalyst. Additionally, the conduction band (CB) potential of Ag_3PO_4 is more +ve than the hydrogen potential (Wang et al., 2012). Thus, electrons

and holes are generated by Ag_3PO_4 by the absorption of a photon, after that a silver atom is produced by the combination of generated electron and interstitial silver ion (Ag^+) leading to the photo-corrosion of Ag_3PO_4 without any sacrificial reagent. The produced suspended Ag particles (black metallic) migrates towards the surface of the Ag_3PO_4 crystal and reduce the catalysts efficiency to absorb visible light which eventually result in decreased photocatalytic activity of Ag_3PO_4 catalyst (Wan et al., 2015).

The insignificant solubility (0.02 g L^{-1}) of Ag_3PO_4 in the solution and its own properties of energy-band structure are responsible for photo-corrosion phenomenon (Tong et al., 2012). Ag_3PO_4 has a conduct band (CB) energy of 0.45 eV, higher than the reduced potential of H_2O/H_2, and if there is no other scavenging agent in the solution the capturing of photo-generated electrons by H_2O would be impossible (Ma et al., 2014). This is the reason that the produced electrons could only be uptake by the interstitial Ag ions leached from the crystal lattice of Ag_3PO_4, and result in accumulation of Ag atom on the surface. This phenomenon

deteriorate the structure of Ag_3PO_4 as well as results in decreased light absorption efficiency of catalyst and eventually reduces its photocatalytic activity and stability (Wang et al., 2012).

2.5. Ag_3PO_4/TiO_2 Composite

The extensive use of TiO_2 photocatalyst is due to its chemical stability, nontoxicity and low cost (Gaya & Abdullah, 2008). Basically, strong oxidizing ability of photo-induced holes by TiO_2 makes it a promising photo-oxidation catalyst, and as compare to other semiconductors, TiO_2 exhibits efficient photo-activity under UV light illumination. But, its activity reduces under visible light irradiation because of large band gap of 3.2

eV. In contrast, photocatalysts having narrow-band gap have the ability to absorb the visible light more efficiently, but their activity and stability requires improvement. That is why, combining TiO_2 with narrow-band gap semiconductors can result in better visible light harvesting and reduces the electron hole recombination by development of well-matched heterogeneous junctions (Rawal, Sung, & Lee, 2012).

Ag_3PO_4 has been reported to effectively harvest visible light for water splitting and organic contaminants degradation (Hu, Wei, Zhang, Zhang, & Li, 2014). A few studies suggest that Ag_3PO_4 shows up to twelve times faster degradation of certain dyes compared to commercially available TiO_2-xNx and $BiVO_4$ with up to 90 % quantum efficiency upon exposure to light with wavelength over 420 nm (Kondo et al., 2008),(Lang, Chen, & Zhao, 2014). However the instability and photo-corrosion of Ag_3PO_4 in aqueous medium has been associated with the loss in photocatalytic efficiency over time making catalyst recycling and reuse difficult (Lazar, Varghese, & Nair, 2012), (Leong et al., 2014). Therefore, it is highly desirable to synthesize modified and stable photocatalysts that can effectively utilize the visible light harnessing power of Ag_3PO_4 nanoparticles with minimal consumption of expensive Ag precursors.

2.6. Self-Corrosion Phenomenon

The photo-induced electrons in the photocatalytic system of Ag_3PO_4 under visible light illumination could combine with the interstitial Ag ion leached from the crystal of Ag_3PO_4 to produce a silver atom, which is owing to the fact that Ag_3PO_4 has a conduct band (CB) energy of 0.45 eV, higher than the reduced potential of H_2O/H_2 (Ma et al., 2014). The produced suspended Ag particles (black metallic) migrates towards the surface of the Ag_3PO_4 crystal and reduce the catalysts efficiency to absorb visible light which eventually result in decreased photocatalytic activity of Ag_3PO_4 catalyst.

Excitedly, the composite of Ag_3PO_4 semiconductor catalyst with TiO_2 shows increased photocatalytic efficiency and stability without any metallic Ag detecting from the XRD pattern of the reacted catalyst.

Self-corrosion phenomenon have a different degree of corrosion than photo-corrosion phenomenon. In this AgO (x = 1, 2) are produced instead of Ag atoms and the composite turns black. Photocatlysis under UV light is independent of self-corrosion phenomenon whether it depends upon adsorption capacity of catalyst, while visible light photocatalysis depends on this phenomenon because of its dependence on amount of light being absorbed. But in general self-corrosion does not reduce photocatalytic efficiency as much as photo-corrosion does that is why Ag_3PO_4/TiO_2 composite is more stable than the bare Ag_3PO_4 catalyst. Moreover, mass spectra (MS) confirmed that the photocatalytic process of the fresh/self-corrosion Ag_3PO_4/TiO_2 and bare TiO_2 is similar. The combination of Ag_3PO_4 with TiO_2 promotes the separation of photo-induced charges and enhances the production of hydroxyl (OH) radicals, thus refining the photocatalytic activity (Ma et al., 2014).

2.7. Immobilization of Nanoparticles

There are two methods of exploiting nanoparticles, either in suspension form or as immobilized on a solid substrate.

2.7.1. Drawbacks of Suspended Nanoparticles

TiO_2 has been extensively used in the form of powder. It can be used for treatment of wastewater in two ways, either in the form suspension or anchored on a solid substrate (Han & Bai, 2009).

- Suspended form has the advantage of large surface area thus exhibits greater photocatalytic efficiency yet it suffers from the following drawbacks:
- Suspended particles have low light utilization efficiency because of the scattering of light rays by the particles. It is reported that at a depth of 0.5 m under the water surface, less than 1% of UV light and almost 20% of visible light actually penetrates.
- Time consuming and expensive post-treatment recovery due to longer settling time requirement of catalyst as well as efficient ultra-filtration techniques (Byrne, Eggins, Brown, McKinney, & Rouse, 1998), (Krýsa, Waldner, Měšťánková, Jirkovský, & Grabner, 2006). It also reduces the reusability of catalyst because of its loss.
- Using suspended particles also found to be unfavourable for human health (Sriwong, Wongnawa, & Patarapaiboolchai, 2008).

2.7.2. Advantages of Immobilized Nanoparticles

Anchorage of suspended particles onto a solid substrate is one of the most effective solution for above mentioned limitations and have several leads such as:

- High quantum utilization efficiency
- Reduced cost and time consumption due to ease of post-treatment recovery
- Enables reuse of catalyst because of low catalyst loss
- Accessibility of longer contact time of the photocatalyst with organic pollutants to be mineralized (Han & Bai, 2009).

2.7.3. Drawbacks of Immobilized Nanoparticles

Immobilization also suffer from some limitations, such as

- Lower surface area availability for reaction (Byrne, Eggins, Brown, McKinney, & Rouse, 1998)
- Properly established and well-defined immobilization methods, techniques and equipment is required as compare to suspended form of TiO_2 which is available in "ready to be used form"
- In general the Overall, the leads of immobilizing TiO_2 compensates the drawbacks and therefore has appealed researchers all over the world to emphasis on inventing simple yet efficient procedures to anchor TiO_2 on solid substrate.

2.8. Immobilization Substrates

Some of the numerous supports that have been reported in the literature are inorganic carbon fabrics, glass mats (Yuranova et al., 2004), synthetic fabrics (Bozzi, Yuranova, & Kiwi, 2005), natural fabrics (Yuranova, Mosteo, Bandara, Laub, & Kiwi, 2006), ITO glass (Sankapal, Lux-Steiner, & Ennaoui, 2005), polymers (Yang, Han, & Choy, 2006), plastics (Kwon, Shin, Kim, Choi, & Yoon, 2004), glass plates, films and fabrics (Zhiyong, Keppner, et al., 2008), hollow glass spheres, quartz optical fibers, reactor walls, fiber glass, polyethylene sheets, silica gel, fly ash, fabric or wool, ceramic membranes and monoliths, micro-porous cellulose membranes, alumina clays, stainless steel, zeolites, anodized iron (Fabiyi & Skelton, 2000).

2.8.1. Characteristics of Good Substrate

A suitable support must have the following characteristics:

- Substrate and photocatalyst must have good affinity for efficient coating
- Immobilization method must not interrupt with the catalytic activity
- The support should be such that, it provides high specific surface area

- Must have capacity to adsorb organic pollutants to be mineralized
- Support and catalyst's binding strength must not be affected by various reaction conditions
- The photocatalyst–substrate must have long term stability

2.8.2. Alumina Beads as Support Substrate

Following characteristics of alumina beads (Al_2O_3) makes it suitable for use as substrate:

- High porosity
- Ease of coating catalyst
- Mechanically Stable
- Thermally stable
- Resistant to Chemicals
- Resistant to UV & visible light
- Inexpensive & readily available

Fig 2.1: Alumina Beads as Immobilization Substrate

2.9. Methods for Immobilization

The technique chosen for attaching particles on the substance significantly affects the photocatalytic activity and that's why be carefully chosen depending on the type of support and the pollutant specie to be mineralized. The immobilization method must not result in any reduction in the photocatalytic activity.

A wide range of techniques have been exploited and reported in the literature. Some of them are spread coating (Shironita et al., 2008), thermal treatment method (Gaya & Abdullah, 2008), chemical vapor deposition (CVD) consisting of atmospheric pressure chemical vapor deposition (APCVD) (Dunnill et al., 2009), sol–gel method (Y. Chen, Stathatos, & Dionysiou, 2008), dip coating methods (Balasubramanian, Dionysiou, Suidan, Baudin, & Laine, 2004), , metal–organic chemical vapour deposition (MOCVD) and hybrid physical chemical vapour deposition (HPCVD), plasma-enhanced chemical vapor deposition (PECVD) (Nizard et al., 2008), sol-spray methods and electrophoretic deposition (Djošić, Mišković-Stanković, Janaćković, Kačarević-Popović, & Petrović, 2006) and Hydrothermal methods (S. Liu & Chen, 2007).

2.10. Phenol (Target Pollutant)

Following are the characteristics of phenol:

- Aromatic Organic Compound
- Also known as Carbolic acid
- Crystalline solid and is volatile
- Phenyl group (-C_6H_5) attached to hydoxyl group (-OH)
- Highly stable
- Tend to bio-accumulate
- Carcinogenic

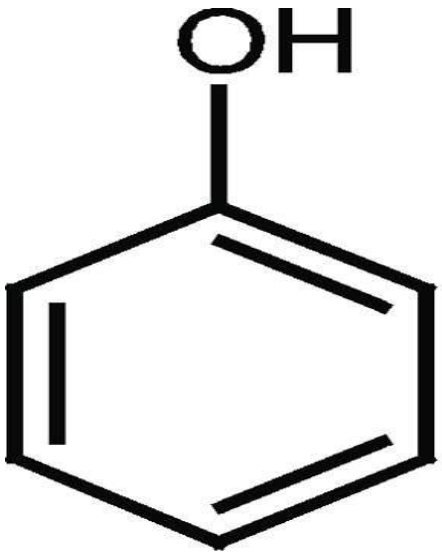

Fig 2.2: Phenol (C_6H_5OH)

2.10.1. Industrial Uses of Phenol

Phenol and its derivatives are used in the production of:

- Plastics
- Polycarbonates
- Epoxides
- Bakelite
- Nylon
- Detergents
- Paints and dyes
- Phenoxy herbicides
- Pharmaceutical drugs

2.10.2. Sources of Phenol

Wastewater of following industries contain phenol and its compounds:

- Oil Refineries

- Pharmaceutical
- Tanneries
- Textile plants
- Food
- Coal processing

2.10.3. Environmental Effects of Phenol

Phenol can be transported by air and water or contaminated products and following are its toxic environmental effects:

- **Acute toxic effects:**
  - Death of animals, birds or fish
  - Death or low growth rate of plants
- **Longer term effects:**
  - Shortened lifespan
  - Reproductive problems
  - Lower fertility
  - Changes in appearance or behavior

2.10.4. Permissible Limits of Phenol

Permissible limit set by Pakistan Environmental Protection Agency (Pak-EPA)

- In inland water: 0.1 mg/L
- In sewage water: 0.3 mg/L
- In sea water: 0.3 mg/L **(Source: Pak-EPA)**

US Environmental Protection Agency (US-EPA) has characterized phenol as priority pollutant (Shet & Shetty K., 2015).

Chapter 3

Materials & Methods

3.1. Materials

Titanium tetra-iso-propoxide (TTIP), Silver nitrate, and Sodium Phosphate (Daejung Korea) were used as precursor for synthesis of TiO_2 nanoparticles, Ag doped titania nanoparticles and Ag_3PO_4/TiO_2 nanoparticles respectively. Alumina beads (Al_2O_3) (Uni-Chem chemical reagents, China) were used as immobilization substrate. Phenol (Merck Germany) was used as model organic pollutant. All chemicals used were of analytical grade and glassware (Pyrex, Germany) was used after rinsing with distilled water. Experiments were repeated three times at least and average values are reported here.

3.2. Synthesis of Titania Nanoparticles

Titanium tetra-iso-propoxide (TTIP) was used as precursor for preparation of TiO_2 nanoparticles via sol gel method (Bahadur et al., 2016). 50 ml of 98% ethanol (AnalaR) was taken in a conical flask and 5 ml of TTIP was added drop wise with continuous stirring. 1-2 drops of nitric acid (Merck Germany) was added to the solution to keep its pH acidic and the solution was kept for stirring for 4 h. The solution was then allowed to settle overnight. The settled particles were then rinsed with distilled water and centrifuged at 5000 rpm for 10 min. This procedure was repeated for 5 times before the particles were kept in oven for 24 h. Finally, the particles were calcined at 450 °C in a muffle furnace (NEY M-525 Series II) for 6 h in order to remove impurities and convert the catalyst into active anatase phase.

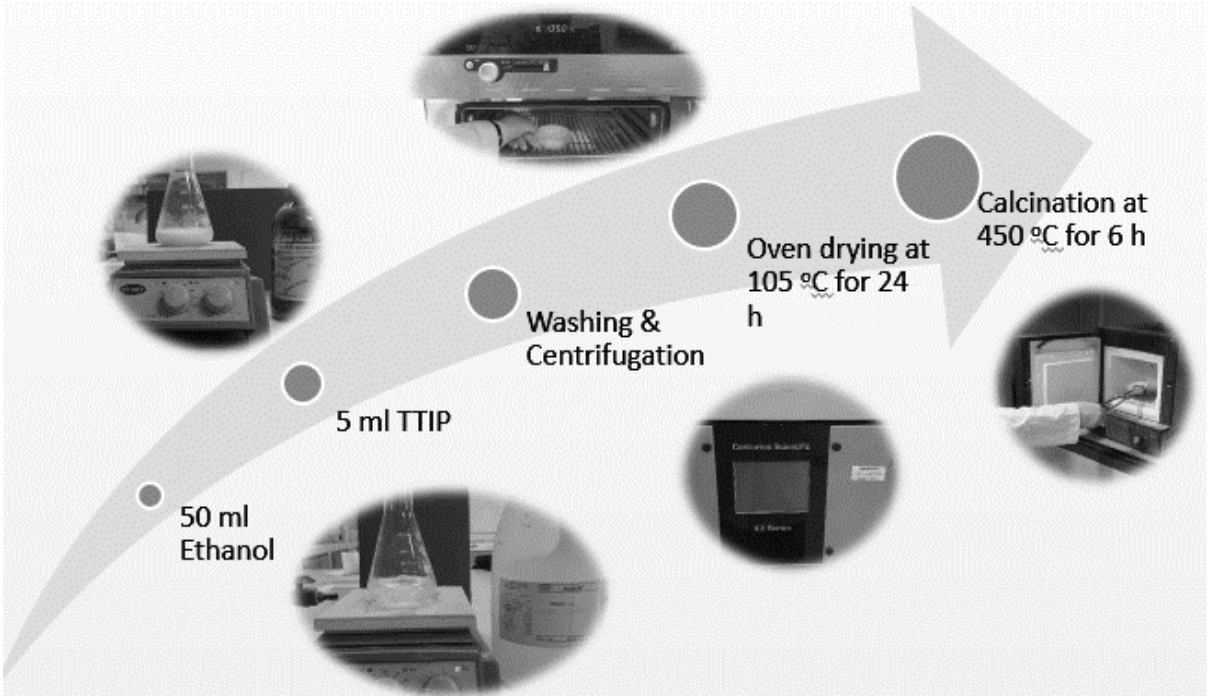

Fig 3.1: Synthesis of Titania (TiO_2) Nanoparticles

3.3. Synthesis of Ag_3PO_4/TiO_2 Nanoparticles

An in-situ precipitation method (Rashid and Barakat, 2014) was adopted for preparation of Ag_3PO_4/TiO_2 nanoparticles. Titania nanoparticles (1.59 g) were dispersed in 50 ml of distilled water and sonicated for 5 min. silver nitrate (3.057 g) was added in the above solution and magnetically stirred for 10 min at 250 rpm. In addition, sodium phosphate (2.13 g) was dissolved in 50 ml of distilled water and then added drop wise to the previously prepared solution. The final solution was then magnetically stirred for 5 h at 250 rpm resulting in a color change from white to yellow. Finally, the solution was filtered, washed and dried in air overnight.

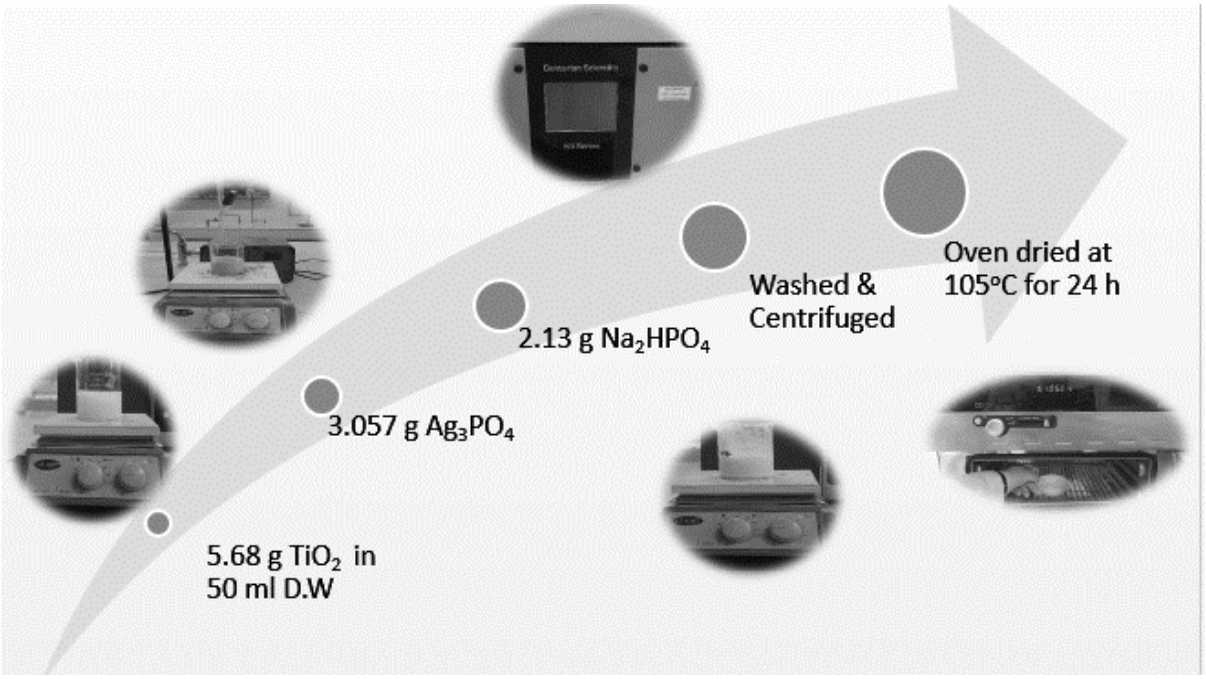

Fig 3.2: Synthesis of Ag_3PO_4/TiO_2 Nanoparticles

3.4. Immobilization of Nanoparticles onto Alumina Beads

Alumina (Al_2O_3) beads were used as supporting material for the immobilization of nanoparticles using heat attachment method (Sakthivel et al., 2002). The TiO_2, Ag doped TiO_2 and, Ag_3PO_4/TiO_2 nanoparticles were coated onto Al_2O_3 beads and labeled as TiO_2-AB, Ag doped TiO_2-AB, and Ag_3PO_4/TiO_2-AB respectively. Initially the alumina beads were dipped in dilute nitric acid for overnight and washed with distilled water. Three grams of each nanoparticle were dispersed in 100 ml of distilled water in respective beakers and sonicated for 10 min. Alumina beads (30 g each) were added to the prepared suspension and magnetically stirred at 300 rpm for 20 min. The mixtures were then dried overnight in an oven at 120 °C. After drying the mixture, it was calcined in muffle furnace at 400 °C for about 2 h in order to remove impurities and enhance the adhesion onto alumina support.

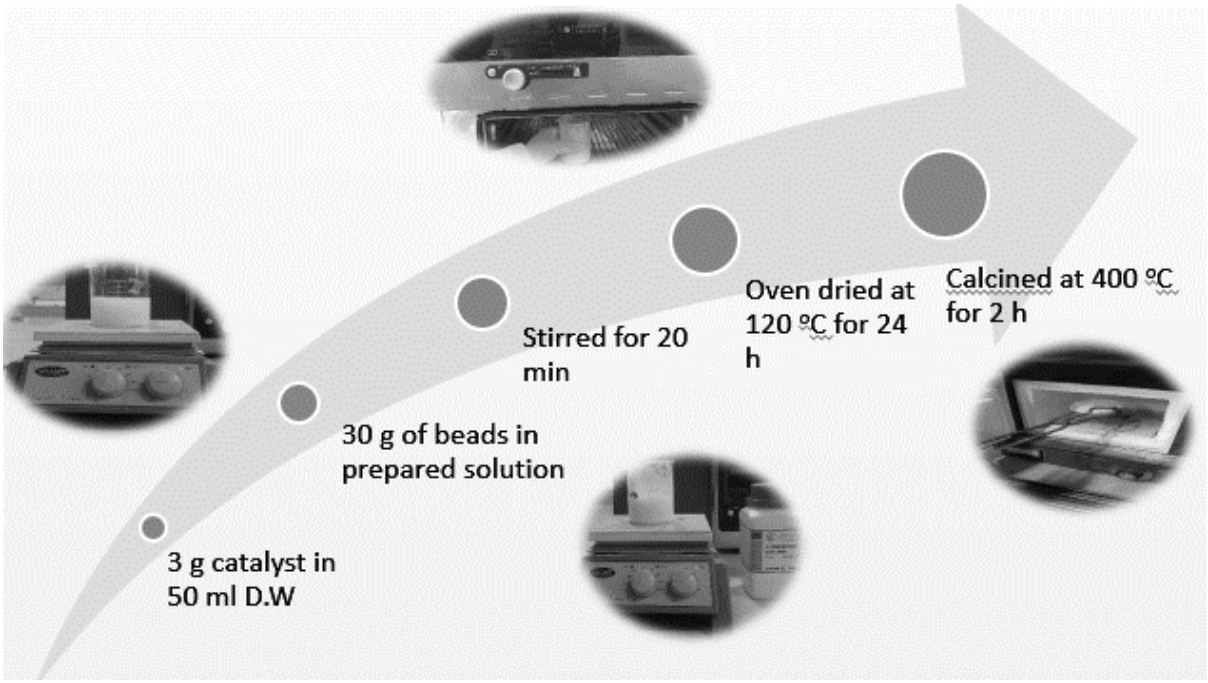

Fig 3.3: Immobilization of Nanoparticles onto Alumina (Al_2O_3) Beads

3.5. Characterization

Samples of three prepared catalysts were characterized by XRD (JEOL JDX-II) with Cu Kα radiation (voltage: 20 kV and current 5 mA) to investigate the crystalline structure of compounds present in each catalyst. Each sample was scanned from a 2θ value of 20° to 80° at a scanning rate of 2°/min and average crystalline size was determined by using Scherrer equation. The MIRA3-TESCAN scanning electron microscope (SEM) was used to study the morphology of uncoated alumina beads as well as alumina beads coated with three prepared catalysts. Both, qualitative and quantitative compositional analyses of the samples were carried out with a microscope equipped with Oxford Energy Dispersive X-ray (EDX) detector. Brunauer–Emmett–Teller (BET) surface areas of the three catalyst samples were studied by N_2 adsorption. Measurements were performed at −196 °C using a TriStar II 3020 sorptometer. Prior to

analysis, samples were degassed at 100 °C under vacuum for 2 h. Surface area was calculated using BET equation

3.6. Experimental Setup

Fig. 3.4 shows the experimental setup used to evaluate the performance of TiO_2-AB, Ag- doped TiO_2-AB, and Ag_3PO_4/TiO_2-AB. A flat-bed photo-reactor, having light source outside was constructed. The reactor was made with acrylic glass sheet (density: 1.18 g/cm^3 and melting point: 160 °C) having dimensions of 25 cm × 10 cm × 5 cm and volume of 1.25 L. Performance of each of the three catalysts was evaluated in three different chambers, i.e. UV, visible and dark. UV and visible chambers were equipped with a UV lamp of 15 W and a fluorescent light of 85 W respectively. Both chambers had adjustable racks facilitating the adjustment of lamp height. Besides, all three chambers had a shaker to place the reactor on. The dark chamber lacked any light source.

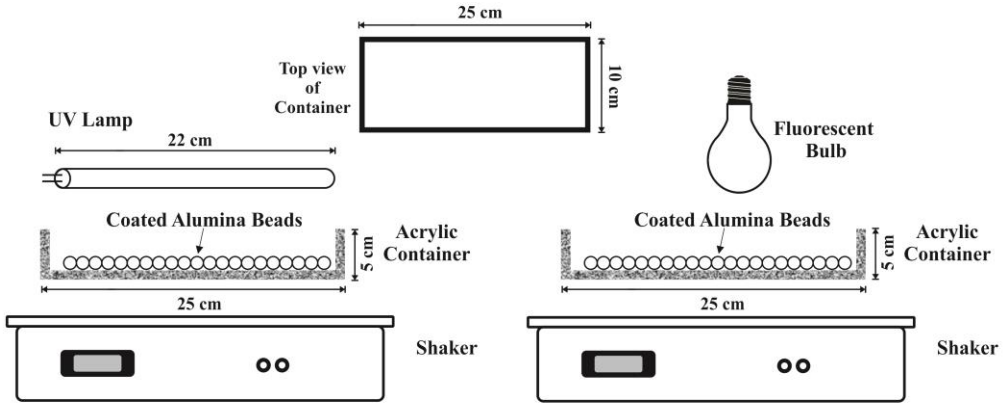

Fig 3.4: Schematic Diagram of Photocatalytic Reactor

In order to perform the experiments, 150 ml of sample (25-100 ppm Phenol) was taken in flat-bed reactor placed on shaker (80 rpm) and the pH of the solution was varied from

4-10 by using 20% HCL and 1N NaOH. Catalyst dose was varied from 30-120 g. The light source was fixed at 10 cm above the sample solution. Degradation was studied for a period of 210 min comprising initial 30 min in dark and a sample of 3 ml was collected after every 60 min for quantification of phenol according to ASTM D-1783 (Test Method B: Direct Photometric) using UV-visible spectrophotometer (PG Instruments Limited, Model no: T60) at a wavelength of 500 nm.

3.7. Adsorption Isotherm Models

The amount of adsorbent required for the adsorption of particular quantity of adsorbate can be defined by the adsorption isotherms in which are one way to understand the adsorption mechanism (Abbas et al., 2016). The three isotherm models Langmuir, Freundlich and Redlich & Peterson (R-P) were used to represent the experimental data of adsorption. The Langmuir isotherm model assumes that the adsorption occurs on a homogenous surface while Freundlich isotherm model describes the adsorption on heterogeneous surface (Abussaud et al., 2016). The R-P isotherm is an empirical model consisting of three parameters having characteristics of both Langmuir and Freundlich isotherm. Three parameters A, B and g (eq. 4) are model constants, and g has the value between 0 and 1 (Behnajady et al., 2014). The isotherm converts to Langmuir and Freundlich isotherm if the value of g=1 and g=0, respectively (Vasanth Kumar and Sivanesan, 2007).

The Langmuir, Freundlich and R-P isotherm models can be mathematically represented by Eq. 1, Eq. 2, and Eq. 3, respectively,

$$q_e = \frac{Q_m K_L C_e}{1 + K_L C_e} \qquad (1)$$

$$q_e = K_F C_e^{\frac{1}{n}} \quad (2)$$

$$q_e = \frac{AC_e}{1 + BC_e^g} \quad (3)$$

where, q_e (mg/g) is equilibrium adsorption capacity of catalyst, C_e (mg/L) is sorbate concentration at equilibrium (liquid phase), Q_m (mg/g) is maximum adsorption capacity, K_L is Langmuir energy constant of adsorption and K_f and n are empirical constants for Freundlich equation. 1/n determines the adsorption intensity and type of isotherm whether they are favorable (1/n < 1) or unfavorable (1/n > 1) (Kumar et al., 2013). A, B and g are the isotherm constants of R-P model.

An error function is usually defined to search for the best fit isotherm model satisfying the experimental adsorption data. In this study, the chi-square test (χ^2) was used for non-linear regression analysis.

3.8. Photo-degradation Kinetic Study

1st order, 2nd order and Langmuir-Hinshelwood kinetic models were used to analyze the transient behavior of photo-degradation kinetics and can be mathematically represented by following Eq. 6, Eq. 8 and Eq. 10.

$$r = -\frac{dC}{dt} = kC_o \quad (5)$$

$$C_e = C_o^{-kt} \quad (6)$$

$$r = \frac{dC}{dt} = kC_o^2 \quad (7)$$

$$C_e = \frac{C_o}{1 + C_o \times kt} \quad (8)$$

$$r = \frac{dC}{dt} = \frac{K_{ad}\, k_{L\text{-}H}\, C_o}{1 + K_{ad}\, C_o} \quad (9)$$

$$C_e = C_o^{-K_{ad} \times (K_{L\text{-}H} + (C_o - C_e))} \quad (10)$$

where, C_e is final concentration, C_o is initial concentration, k is rate constant (slope), t is time, $k_{L\text{-}H}$ is rate constant and K_{ad} is adsorption equilibrium constant.

Chapter 4

Results and Discussion

4.1. Characterization

The XRD pattern of the pure TiO_2, Ag-doped-TiO_2 and Ag_3PO_4/ TiO_2 composite is shown in the Fig. 4.1 Pure TiO_2 displays a strong peak at 25.24° corresponding to the (1 0 1) plane of anatase phase with subsequent peaks at 36.90°, 37.72°, 38.53°, 47.99°, 53.82°, 54.97°, 62.04°, 62.60°, 68.75°, 70.27°, and 74.96° (Ahmad et al., 2017). The dominant peaks of Ag_3PO_4/TiO_2 composite at 33.3°and 36.6° can be indexed to (2 1 0) and (2 1 1) planes, respectively (Li et al., 2013). In the diffraction pattern of Ag-TiO_2 catalyst, the peak of Ag could not be observed as Ag loading on TiO_2 is less than 5 wt% (Altın and Sökmen, 2014). The crystallite average sizes of TiO_2, Ag-TiO_2 and Ag_3PO_4/TiO_2 nanoparticles were also calculated using the Scherrer equation (Mehmood et al., 2015). The calculated crystallite sizes for TiO_2, Ag-TiO_2 and Ag_3PO_4/TiO_2 composites were 48.4, 48.7 and 44.4 nm, respectively.

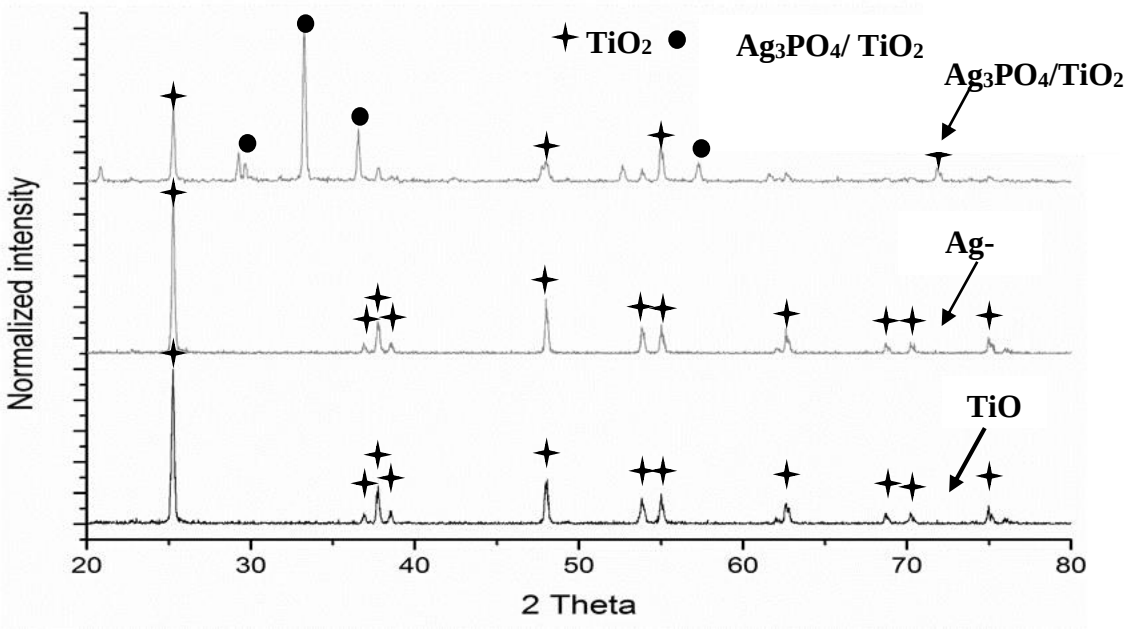

Fig 4.1: XRD pattern of TiO_2, Ag-TiO_2 and Ag_3PO_4/TiO_2 composites

The SEM images of uncoated and coated alumina (Al_2O_3) beads are shown in Fig. 4.2 From the image a, it can be seen that Al_2O_3 bead is highly porous and have large surface area thus providing suitable substrate for the anchorage of particles. The EDS results shown in Fig. 4.3 indicate considerable amount of coating on the beads.

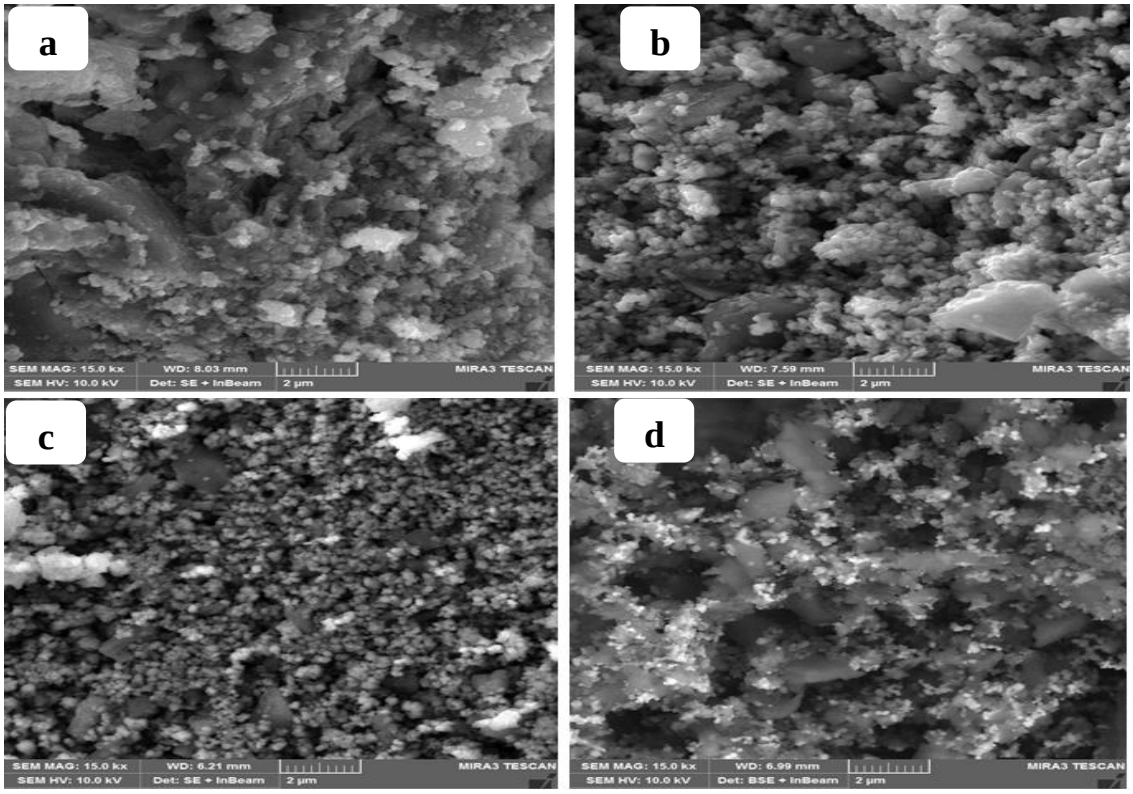

Fig 4.2: SEM Images of (a) Un-coated bead, (b) TiO_2 coated bead, (c) Ag-TiO_2 coated bead, (d) Ag_3PO_4/TiO_2 coated bead

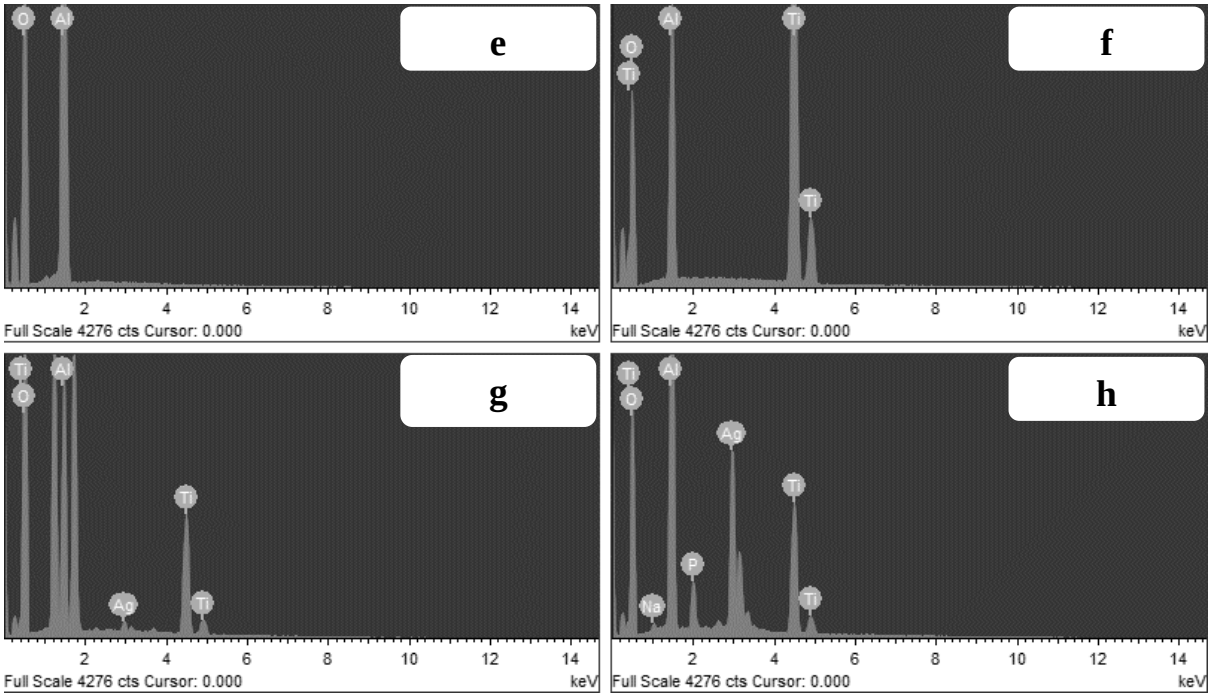

Fig 4.3: EDS Images of (e) Un-coated bead, (f) TiO_2 coated bead, (g) Ag-TiO_2 coated bead, (h) Ag_3PO_4/TiO_2 coated bead

In addition, BET characterization of TiO_2, Ag-TiO_2 and Ag_3PO_4/TiO_2 catalyst was performed to find the surface area as shown in Table 4.1 Highest surface area of 51.59 m^2/g was found for Ag_3PO_4/TiO_2 composite as compared to other two catalysts, Ag-TiO_2 (44.11 m^2/g) and TiO_2 (40.89 m^2/g).

Table 4.1: BET Characteristic Data of TiO_2, Ag-TiO_2 and Ag_3PO_4/TiO_2

Catalyst	Surface Area (m^2/g)	Pore Volume (cm^3/g)	Pore Size (Å)
TiO_2	40.89	0.039	47.75
Ag-TiO_2	44.10	0.042	46.08
Ag_3PO_4/TiO_2	51.59	0.056	43.81

4.2. Catalyst Performance Evaluation

The performance evaluation of catalyst for the photocatalysis process was carried on TiO_2-AB as reference catalyst. The effect of variation in pH of pollutant solution,

catalyst dose and initial phenol concentration were analyzed on the photo-degradation of Phenol. The performance of Ag-doped TiO_2-AB, and Ag_3PO_4/TiO_2-AB was evaluated on the set of pH, catalyst dose and pollutant concentration parameters for which the TiO_2-AB performed the best.

4.2.1. Effect of pH

Many catalysts and substrates act as both acid and base resulting in different surface charge under various pH conditions (Sakthivel et al., 2002). The effect of pH on phenol degradation was studied in three mediums, acidic (pH 4), basic (pH 10) and solution's natural pH (pH 7.3). The other parameters initial concentration, catalyst dose and contact time were kept constant at 25ppm, 30g/150mL and 210 min. Fig. 4.4 shows the results for effect of pH on phenol degradation. The phenol degradation increases with a decrease in pH and the maximum value was obtained at pH 4. The pH greater than pH_{PZC} (Point of Zero Charge) results in the negatively charged surface which is suitable for the adsorption of more positive organic pollutants because of strong interactions (Atieh et al., 2010). TiO_2 and Al_2O_3 have 6.8 and 9.1 point of zero charge, respectively. TiO_2 immobilized Al_2O_3 catalyst have a positive charge at acidic pH while they are more negative at basic pH (Sakthivel et al., 2002) thus enhancing the electrostatic attraction between catalyst and anionic phenol. Similar effect of pH on TiO_2 and phenol degradation was reported by S.H. Lin., et al (Lin et al., 2011b).

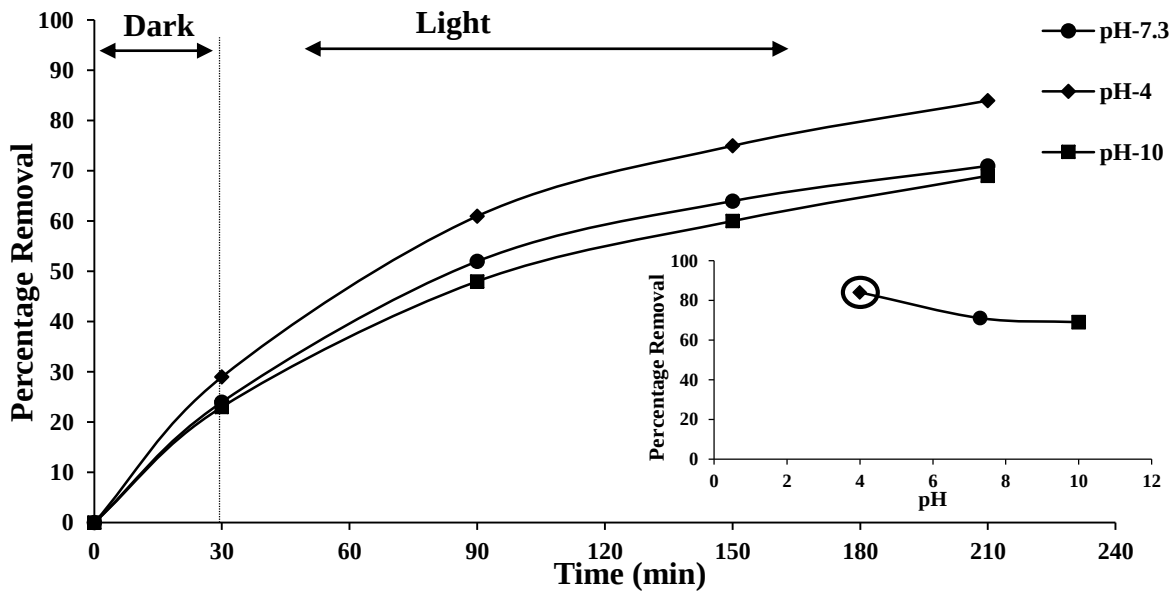

Fig 4.4: Effect of pH on degradation of phenol (initial concentration: 25 ppm, catalyst dose: 30 g/150 ml, contact time: 210 min and temperature: 25 °C)

4.2.2. Effect of catalyst dose

The quantity of catalyst specie is yet another important parameter to be considered in degradation study. In this work the catalyst is supported on a substrate and their combined weight is considered as dose. Each uncoated substrate (Al_2O_3) bead weighs around 0.203 g. To analyze the effect of catalyst dose on rate of catalysis, four different doses 30 g/150 ml, 60 g/150 ml, 90 g/ ml and 120 g/ 150 ml with other conditions being constant pH: 4, initial concentration: 25 ppm and contact time: 210 min were selected. Results of the analysis are shown in Fig. 4.5 Increasing the catalyst dose results in increased rate of removal and a maximum of 96% removal efficiency was achieved with 90 g/150 ml dose in 210 min of catalysis, beyond this, no significant increase in removal rate was observed (Hosseini et al., 2007). This can be attributed to the low utilization of light because of overlapping of substrate layers. 90 g coated alumina beads forms a uniform layer at the base of reactor, when the catalyst dose increased from 90 to 120 g another layer starts to form. Now this new upper layer is active because of

maximum adsorption of light and the layer beneath will remain inactive, thus resulting in constant rate of degradation.

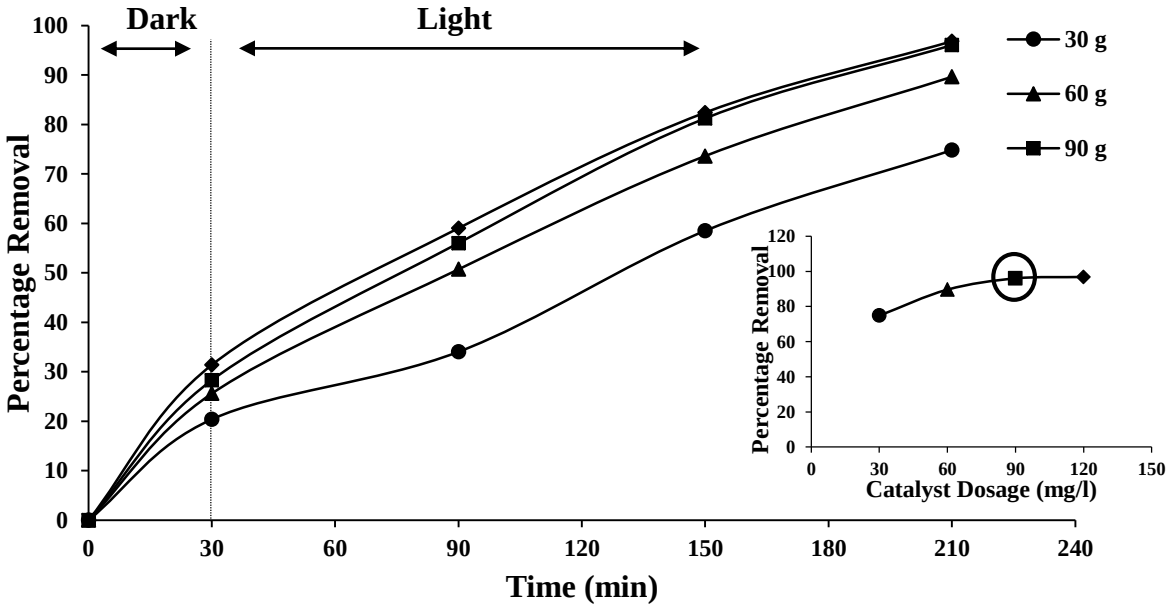

Fig 4.5: Effect of Catalyst Dose on degradation of phenol (pH: 4, initial concentration: 25 ppm, contact time: 210 min and temperature: 25 °C)

4.2.3. Effect of initial concentration of Phenol

In order to evaluate the effect of phenol's initial concentration on degradation, various concentrations 25ppm, 50 ppm, 75 ppm and 100 ppm at pH: 4 catalyst dose: 90 g/ 150ml were tested. Fig. 4.6 represents the obtained results. Rise in phenol's concentration retards the removal efficiency and results in 31% decrease in removal efficiency when the concentration increased from 25 ppm to 100 ppm in 210 min. The photocatalyst produces the •OH and O_2 radicals which react with the pollutant molecules being adsorbed on the surface of catalyst. As the catalyst dose (90 g/150 ml) is fixed so the active sites and production of •OH and O_2 radicals will be restricted. Now increasing the initial concentration of the pollutant will decrease the probability

of pollutant molecules to react with •OH and O_2 radicals because of the limited production of •OH and O_2 radicals and hence decreases the degradation efficiency. Therefore at higher initial concentrations of pollutant, the molecules will have to compete for their active sites and for the provision of the •OH and O_2 radicals; thus, the rate of degradation reduces (Kashif and Ouyang, 2009).

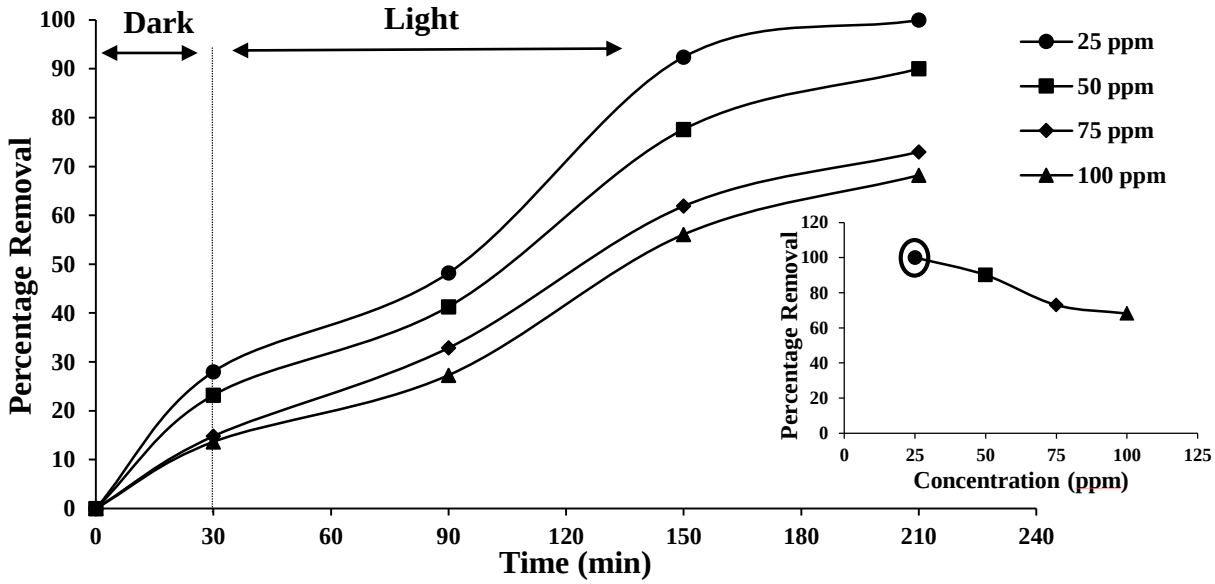

Fig 4.6: Effect of Initial Concentration degradation of phenol (pH: 4, catalyst dose: 90 g/150 ml, contact time: 210 min and temperature: 25 °C)

4.2.4. Photocatalysis under UV and Visible light

The efficiency of the three prepared catalysts was tested for degradation of phenol under both UV and visible irradiation. Since the substrate and catalyst have adsorption capability which can affect the photocatalytic activity, the adsorbed amount of phenol on catalysts was measured in dark. After establishing the adsorption-desorption equilibrium the solution containing phenol was illuminated to light source and relative concentration of phenol was measured at equal intervals. Fig. 4.7a and b show the degradation of phenol under both UV and visible light respectively. The best results

were obtained from Ag_3PO_4/TiO_2 catalyst in both sources of light. The other two catalysts TiO_2 and Ag-TiO_2 also showed some degradation but required more time for complete degradation. This can be attributed to the large surface area and high adsorption capacity of Ag_3PO_4/TiO_2 catalyst as confirmed by the BET analysis and adsorption kinetic model.

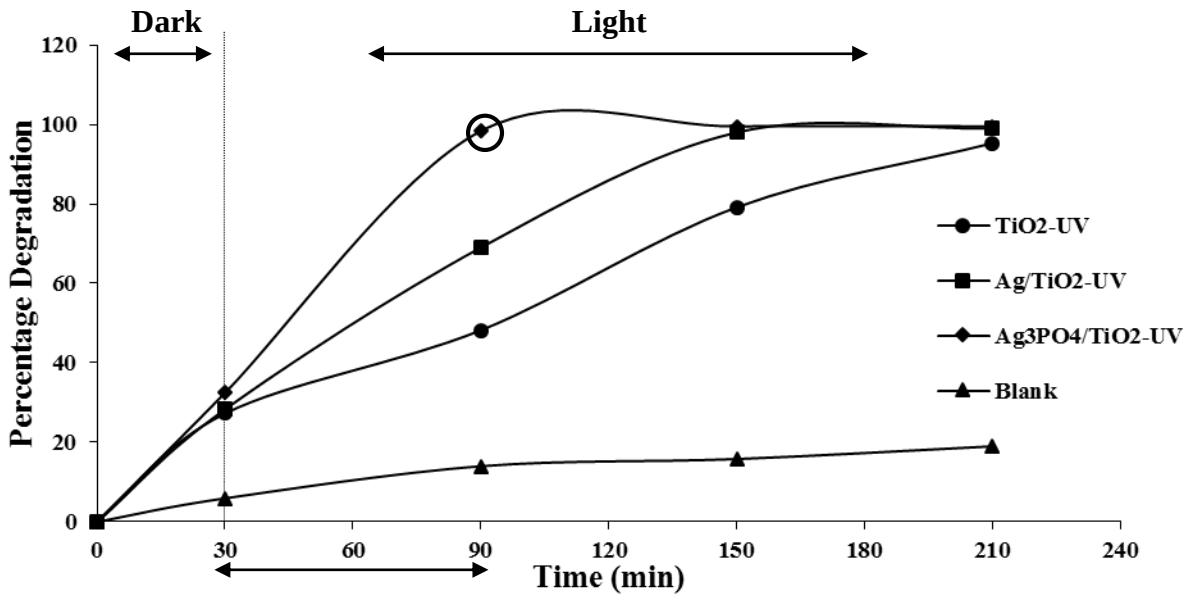

(a)

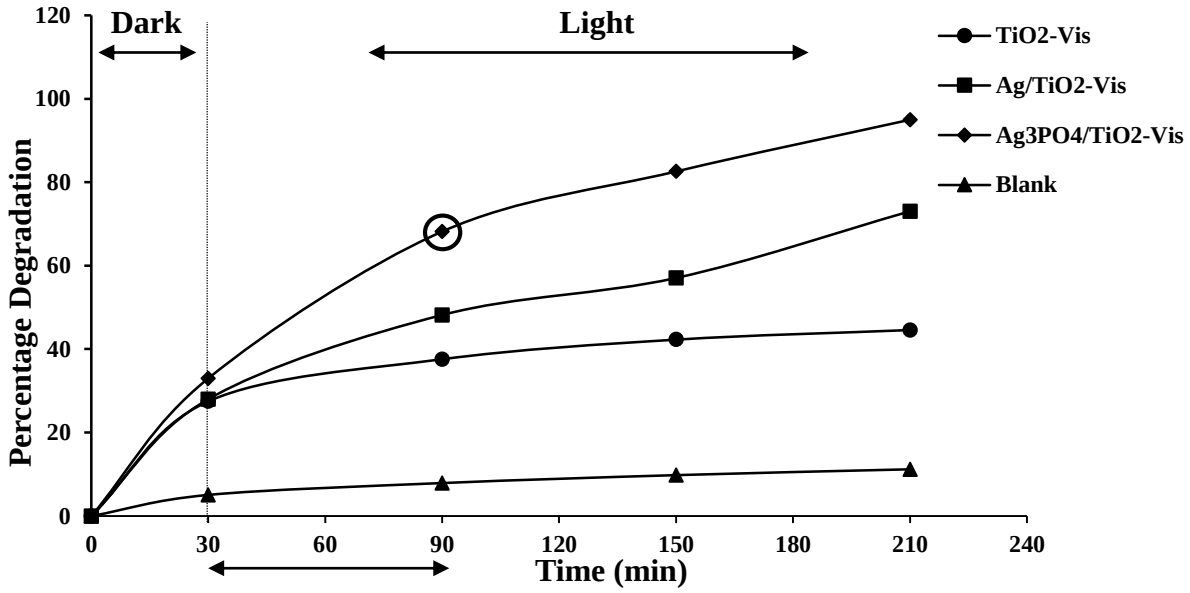

(b)

Fig 4.7: Photocatalysis of Phenol under (a) UV light (b) Visible Light (pH: 4, initial concentration: 25 ppm, catalyst dose: 90 g/150 ml, contact time: 210 min and temperature: 25 °C)

4.3. Adsorption Isotherm Models

The experimental results obtained for the adsorption of phenol were analysed by the Langmuir, Freundlich and Redlich-Peterson (R-P) isotherm models using non-linear regression analysis. The non-linear form of Langmuir, Freundlich and R-P isotherm model is given by Eq. (1), (2) and (3) while a plot of q_e (mg/g) against C_e (mg/l) is shown in Fig. 4.8a, b and c for TiO_2, Ag-TiO_2 and Ag_3PO_4/TiO_2 respectively. (Abussaud et al., 2016).

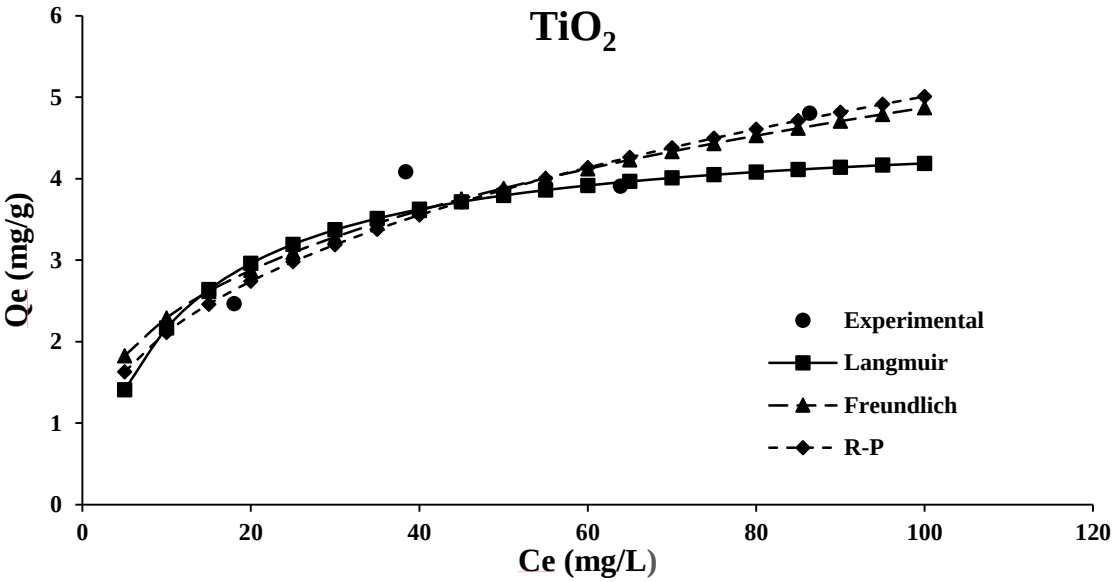
TiO2
Qe (mg/g)
Ce (mg/L)
Experimental
Langmuir
Freundlich
R-P
0
1
2
3
4
5
6
0
20
40
60
80
100
120

(a)

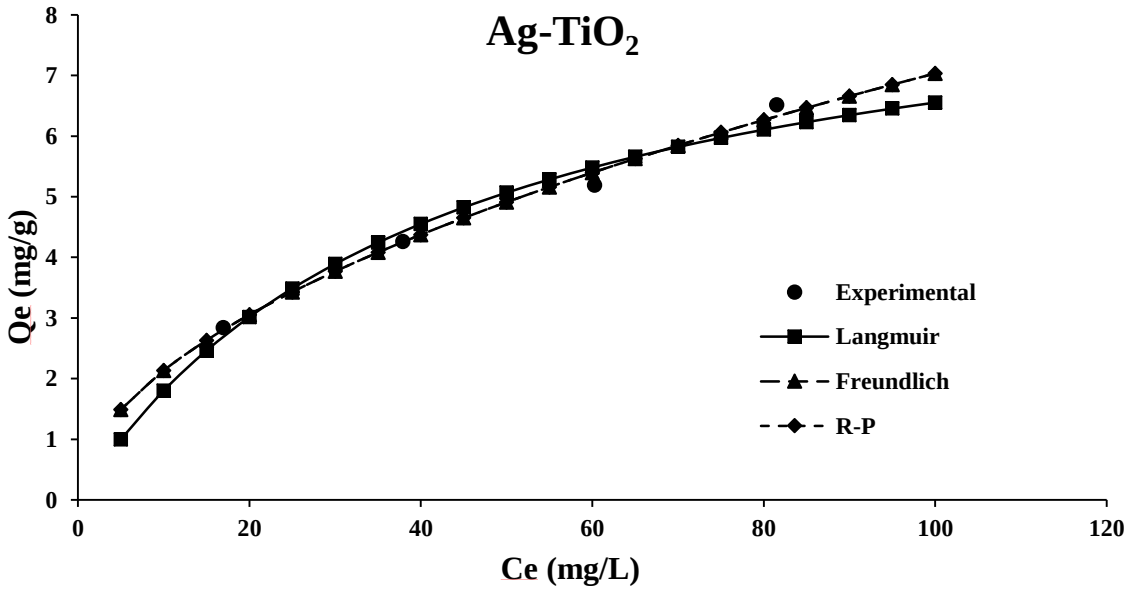
Ag-TiO2
Qe (mg/g)
Ce (mg/L)
Experimental
Langmuir
Freundlich
R-P
0
1
2
3
4
5
6
7
8
0
20
40
60
80
100
120

(b)

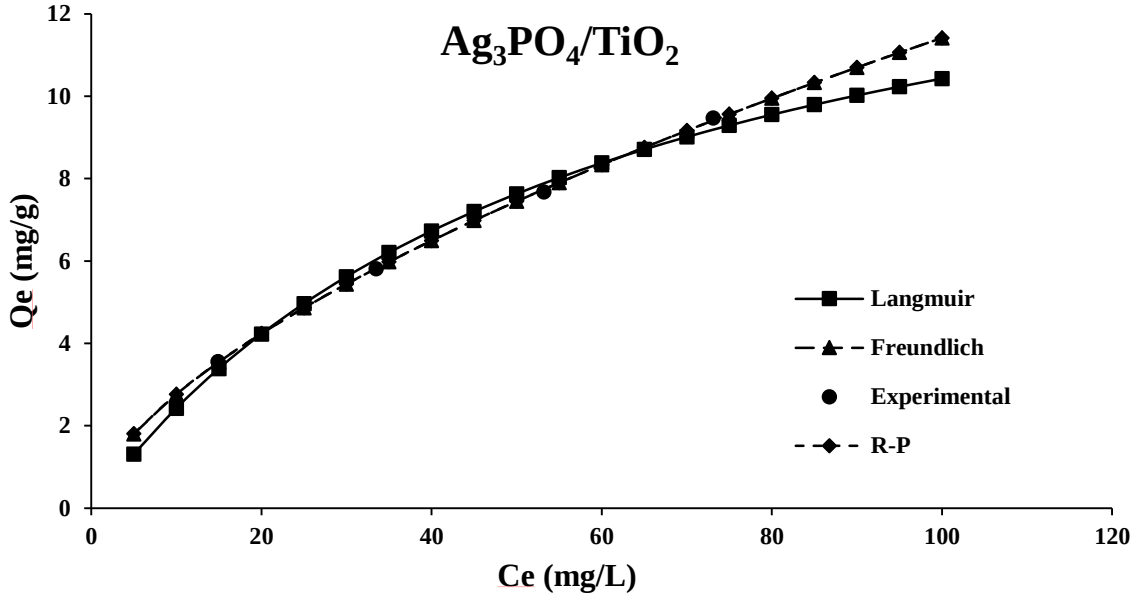

(c)

Fig 4.8: Isotherm Models for (a) TiO_2, (b) Ag-TiO_2 and (c) Ag_3PO_4/TiO_2

It was observed that a good straight line for both Freundlich and R-P model with lowest chi square (χ^2) value was obtained for TiO_2, Ag-TiO_2 and Ag_3PO_4/TiO_2 coated alumina (Al_2O_3) beads. The adsorption behaviour of adsorbent was best described by Freundlich and R-P isotherm models as shown by their χ^2, 1/n and g values in the Table 4.2.

Table 4.2: Adsorption Isotherm model parameters using non-linear regression analysis

TiO_2		**Ag-TiO_2**	**Ag_3PO_4-TiO_2**
Langmuir Model			
q_m (mg/g)	4.67	9.28	16.48
K_L (L/mg)	0.09	0.02	0.01
Chi sq (χ^2)	0.21	0.05	0.03

Freundlich Model			
N	3.05	1.93	1.62
1/n	0.33	0.52	0.62
K_F (L/mg)	1.08	0.64	0.67
Chi sq (χ^2)	0.14	0.02	0.001
Redlich-Peterson Model			
B	2659.84	3061.61	2970.68
A (L/g)	2373.53	1976.74	1991.18
g (L/mg)	0.63	0.48	0.38
Chi sq (χ^2)	0.12	0.012	0.001

4.4. Photo-degradation Kinetic Models

Chi-square statistics (χ^2) was used to determine the non-linear best fit photocatalysis kinetic model. The lower value of χ^2determines the best fit kinetic model for photocatalytic degradation (Ho et al., 2005). The χ^2 and parameter values for 1st order, 2nd order and Langmuir–Hinshelwood (L-H) model are presented in the Table 4.3 and 4.4. Fig. 4.9 and 4.10 show photo-degradation kinetic models for TiO_2, Ag-TiO_2 and Ag_3PO_4/TiO_2 under UV and visible light respectively. In this study, for all catalysts, L-H model considered to be a best fit photo kinetic model due to lower value of χ^2 for all three catalysts as compared to 1st and 2nd order kinetics. While the two parameters of

L-H model, K_{ads} and K_{L-H} suggest the rate determining step in photo-degradation experiments (Bhattacharyya et al., 2004). In L-H model the value of photocatalytic rate constant (K_{L-H}) is greater than the adsorption rate constant (K_{ads}) for all prepared catalysts (TiO_2, Ag-TiO_2 and Ag_3PO_4/TiO_2). It would be suggested that photocatalysis is the rate determining step in the photo-degradation of phenol dye (Li et al., 2006).

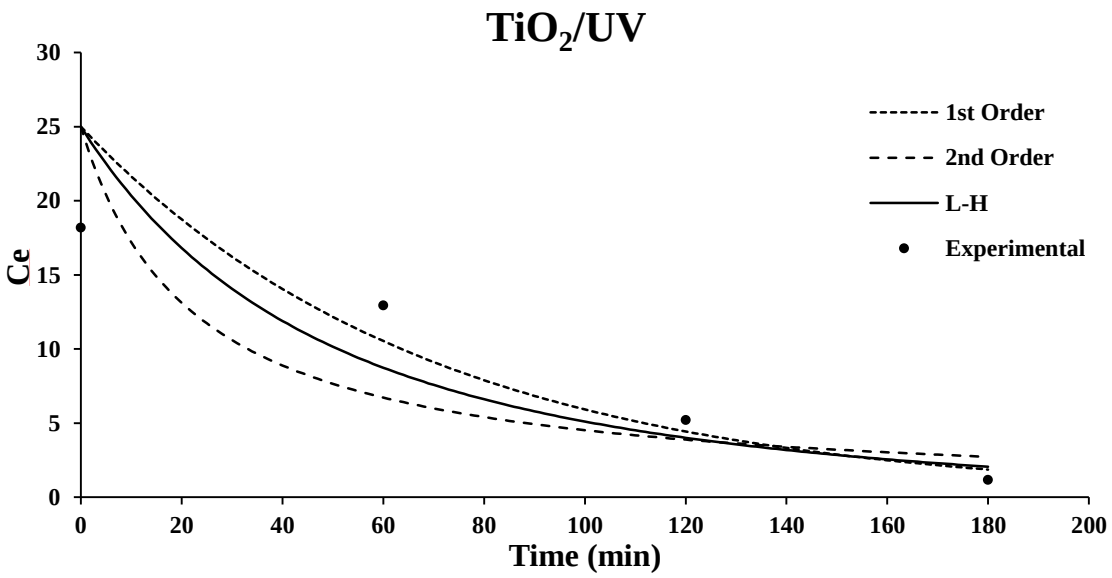

(a)

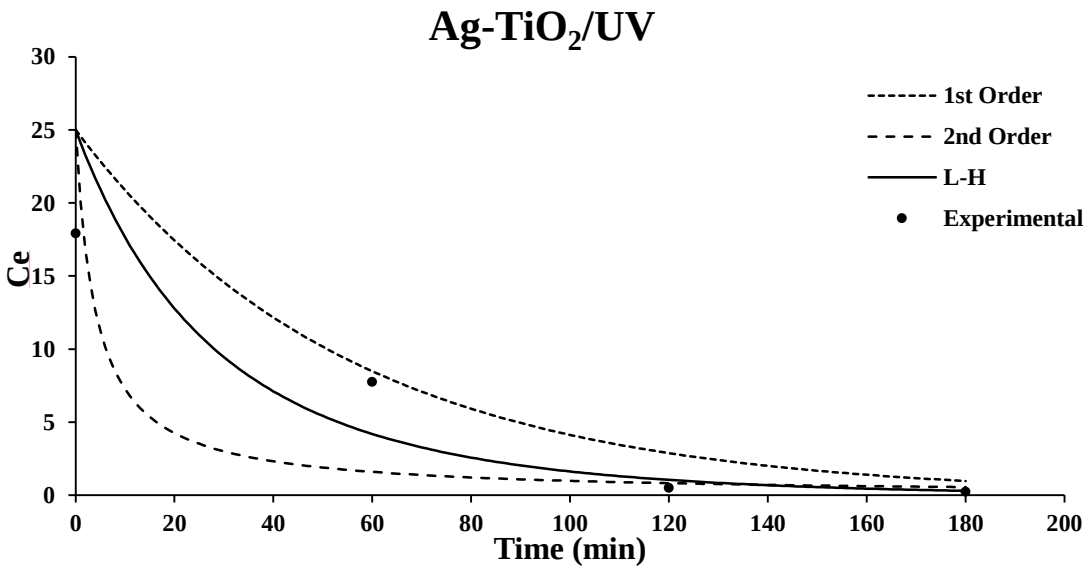

(b)

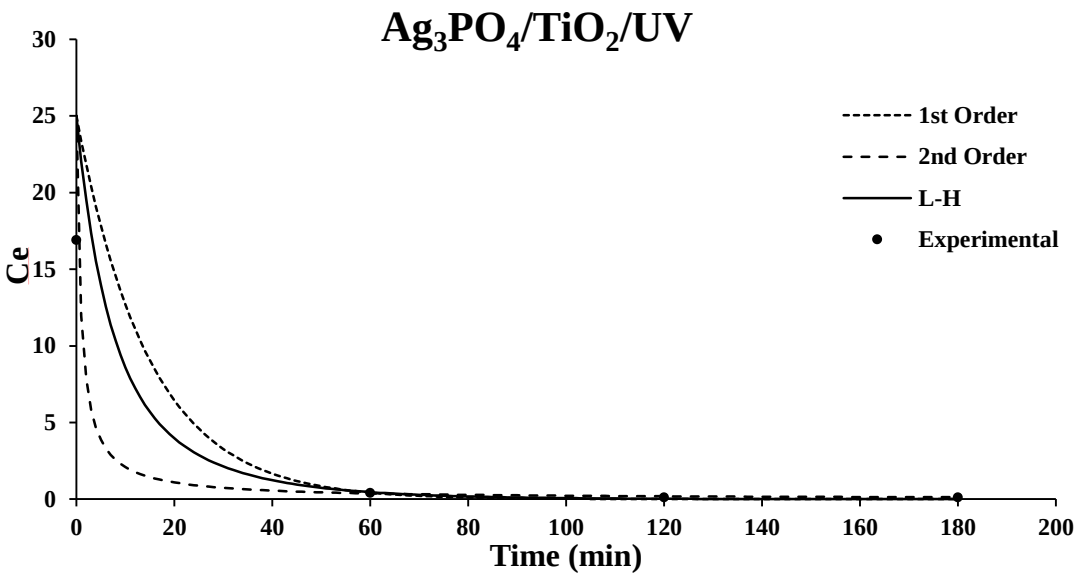

(c)

Fig 4.9: Photo-degradation Kinetic Models of (a) TiO_2/UV (b) Ag-TiO_2/UV (c) Ag_3PO_4/TiO_2/UV

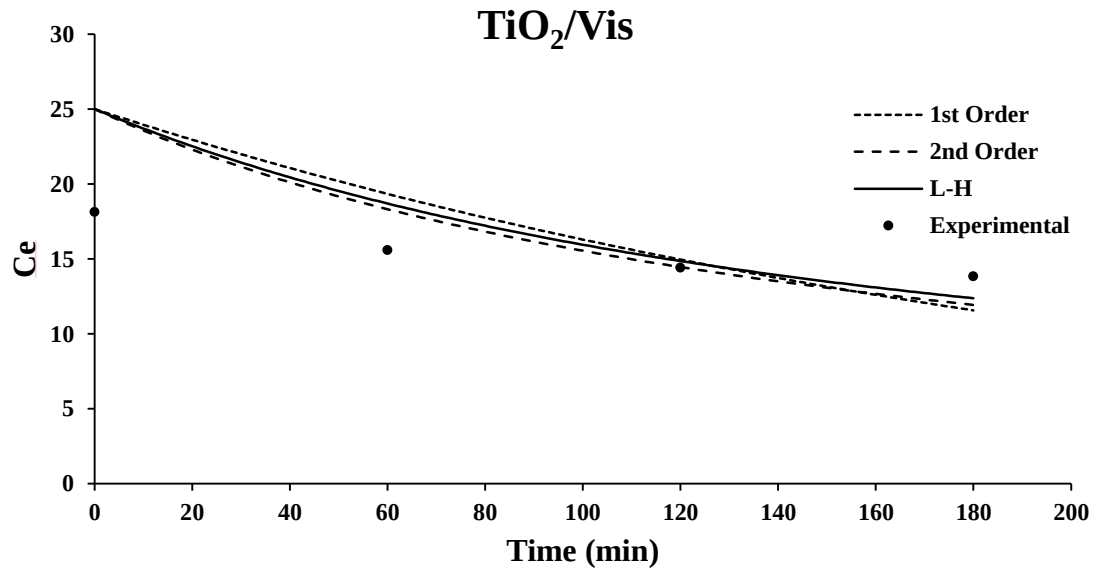

(a)

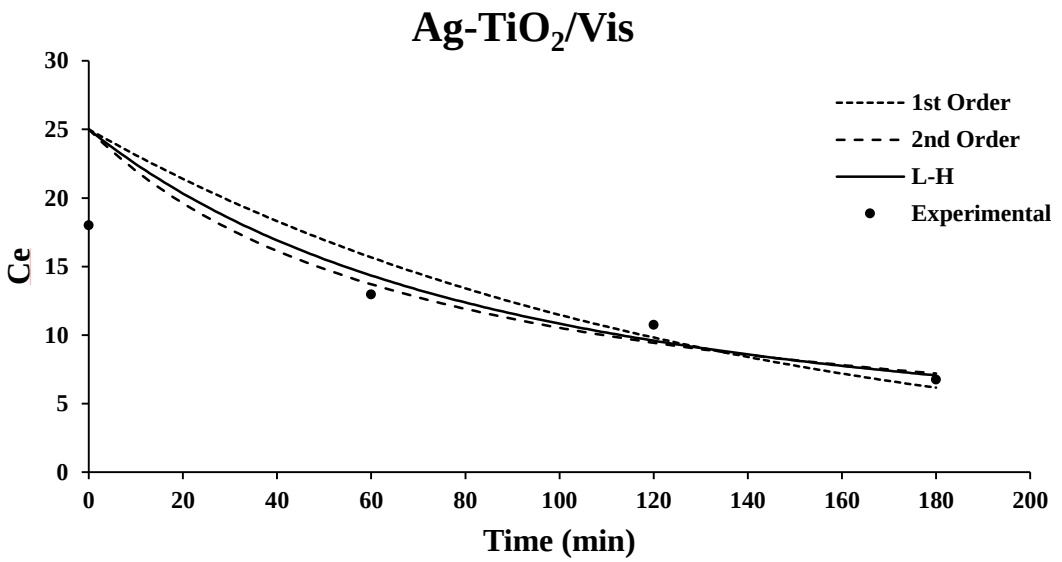

(b)

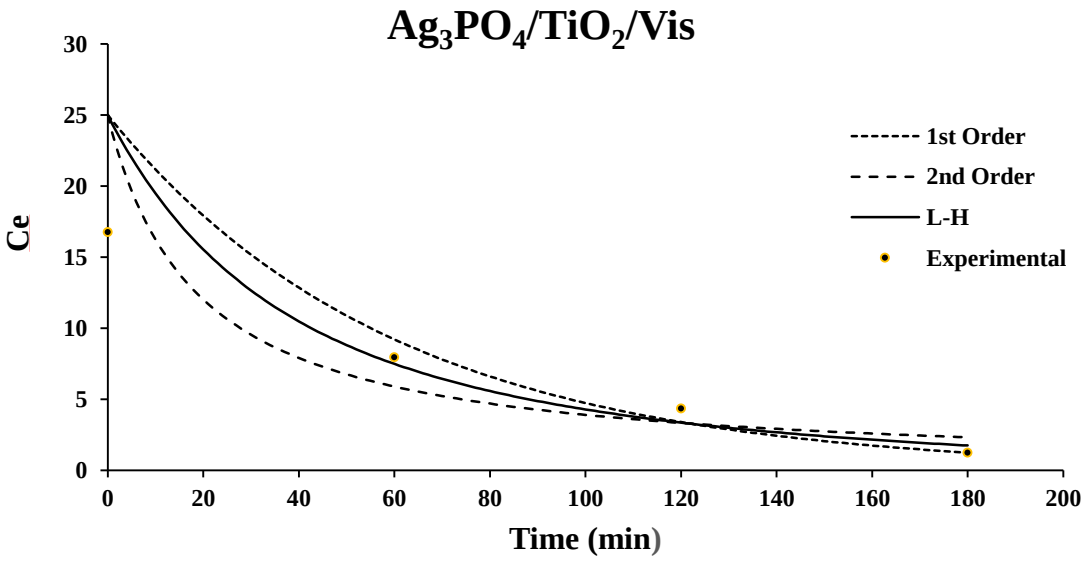

(c)

Fig 4.10: Photo-degradation Kinetic Models of (a) TiO_2/Vis (b) Ag-TiO_2/Vis (c) Ag_3PO_4-TiO_2/Vis

Table 4.3: Photo-degradation Kinetic Model Parameters (under UV Light)

	TiO_2	Ag-TiO_2	Ag_3PO_4/TiO_2
1st Order			
k	0.01	0.01	0.02
R^2	0.89	0.98	0.99
Chi sq (χ^2)	3.89	3.42	4.47
2nd Order			
k	0.0002	0.001	0.002
R^2	0.74	0.85	0.99
Chi sq (χ^2)	3.34	2.95	5.76
Langmuir-Hishelwood			
k	0.05	0.04	0.04
K_{L-H}	0.01	0.06	0.23
R^2	0.91	0.94	0.99
Chi sq (χ^2)	0.001	0.10	0.53

Table 4.4: Photo-degradation Kinetic Model Parameters (under Visible Light)

	TiO_2	Ag-TiO_2	Ag_3PO_4/TiO_2
1st Order			
k	0.01	0.02	0.07
R^2	0.96	0.97	0.98
Chi sq (χ^2)	3.52	6.37	4.40
2nd Order			
k	0.002	0.01	0.01
R2	0.99	0.93	0.92
Chi sq (χ^2)	7.92	8.26	3.92
Langmuir-Hishelwood			
k	0.03	0.04	0.05
K_{L-H}	0.30	0.53	0.96
R^2	0.99	0.98	0.98
Chi sq (χ^2)	1.96	2.27	0.19

Chapter 5

Conclusions & Recommendations

5.1. Conclusions

From the research work described above, it is concluded that:

1. High porosity of alumina beads make them suitable substrate for immobilization
2. Ag_3PO_4/TiO_2 Composite exhibits the highest efficiency under both UV and Visible light irradiation as compare to TiO_2 & Ag-doped-TiO_2
3. The data from the phenol adsorption by prepared photocatalysts TiO_2, Ag-doped-TiO_2 and Ag_3PO_4/ TiO_2 was best fitted by both Langmuir and Freundlich Isotherm Models and 1st Order Kinetic Model
4. The concentration of phenol was effectively reduced

5.2. Recommendations

Following are some of the suggestions for carrying forward the work reported in this thesis:

1. Different types of substrates need to be evaluated in case of Ag_3PO_4/TiO_2 composite
2. As Ag_3PO_4/TiO_2 composite is visible light active that's why solar light can be directly or indirectly (using solar panels) utilized making the process energy efficient
3. The efficiency of Ag_3PO_4/TiO_2-AB catalyst needs to be exploited for degradation of other organic pollutants
4. Further study is required to minimize the effect of self-corrosion phenomenon of Ag_3PO_4/TiO_2 composite

References

1. Abou-Gamra, Z. M., & Ahmed, M. A. (2015). TiO_2 nanoparticles for removal of malachite green dye from waste water. Advances in Chemical Engineering and Science, 5(03), 373.
2. Balasubramanian, G., Dionysiou, D. D., Suidan, M. T., Baudin, I., & Laîné, J. M. (2004). Evaluating the activities of immobilized TiO_2 powder films for the photocatalytic degradation of organic contaminants in water. Applied Catalysis B: Environmental, 47(2), 73-84.
3. Basha, S., Keane, D., Morrissey, A., Nolan, K., Oelgemöller, M., & Tobin, J. (2010). Studies on the adsorption and kinetics of photodegradation of pharmaceutical compound, Indomethacin using novel photocatalytic adsorbents (IPCAs). Industrial & Engineering Chemistry Research, 49(22), 11302-11309.
4. Bi, Y., Ouyang, S., Cao, J., & Ye, J. (2011). Facile synthesis of rhombic dodecahedral AgX/Ag_3PO_4 (X= Cl, Br, I) heterocrystals with enhanced photocatalytic properties and stabilities. Physical Chemistry Chemical Physics, 13(21), 10071-10075.
5. Bi, Y., Ouyang, S., Cao, J., & Ye, J. (2011). Facile synthesis of rhombic dodecahedral AgX/Ag 3 PO 4 (X= Cl, Br, I) heterocrystals with enhanced photocatalytic properties and stabilities. Physical Chemistry Chemical Physics, 13(21), 10071-10075.
6. Bozzi, A., Yuranova, T., & Kiwi, J. (2005). Self-cleaning of wool-polyamide and polyester textiles by TiO_2-rutile modification under daylight irradiation at ambient temperature. Journal of Photochemistry and Photobiology A: Chemistry, 172(1), 27-34.

7. Byrne, J. A., Eggins, B. R., Brown, N. M. D., McKinney, B., & Rouse, M. (1998). Immobilisation of TiO_2 powder for the treatment of polluted water.Applied Catalysis B: Environmental, 17(1), 25-36.
8. Chen, X., Dai, Y., & Wang, X. (2015). Methods and mechanism for improvement of photocatalytic activity and stability of Ag_3PO_4: A review. Journal of Alloys and Compounds, 649, 910-932.
9. Chen, Y., Stathatos, E., & Dionysiou, D. D. (2008). Microstructure characterization and photocatalytic activity of mesoporous TiO_2 films with ultrafine anatase nanocrystallites. Surface and Coatings Technology,202(10), 1944-1950.
10. Dhananjeyan, M. R., Kiwi, J., Albers, P., & Enea, O. (2001). Photo-Assisted Immobilized Fenton Degradation up to pH 8 of Azo Dye Orange II Mediated by Fe3+/Nafion/Glass Fibers. Helvetica Chimica Acta, 84(11), 3433-3445.
11. Djošić, M. S., Mišković-Stanković, V. B., Janaćković, D. T., Kačarević-Popović, Z. M., & Petrović, R. D. (2006). Electrophoretic deposition and characterization of boehmite coatings on titanium substrate. Colloids and Surfaces A: Physicochemical and Engineering Aspects, 274(1), 185-191.
12. Dunnill, C. W., Aiken, Z. A., Pratten, J., Wilson, M., Morgan, D. J., & Parkin, I. P. (2009). Enhanced photocatalytic activity under visible light in N-doped TiO_2 thin films produced by APCVD preparations using t-butylamine as a nitrogen source and their potential for antibacterial films. Journal of Photochemistry and Photobiology A: Chemistry, 207(2), 244-253.
13. Fabiyi, M. E., & Skelton, R. L. (2000). Photocatalytic mineralisation of methylene blue using buoyant TiO_2-coated polystyrene beads. Journal of Photochemistry and Photobiology A: Chemistry, 132(1), 121-128.

14. Fu, J., Chen, Z., Wang, M., Liu, S., Zhang, J., Zhang, J., & Xu, Q. (2015). Adsorption of methylene blue by a high-efficiency adsorbent (polydopamine microspheres): kinetics, isotherm, thermodynamics and mechanism analysis. Chemical Engineering Journal, 259, 53-61.
15. Gaya, U. I., & Abdullah, A. H. (2008). Heterogeneous photocatalytic degradation of organic contaminants over titanium dioxide: a review of fundamentals, progress and problems. Journal of Photochemistry and Photobiology C: Photochemistry Reviews, 9(1), 1-12.
16. Guo, J., Ouyang, S., Li, P., Zhang, Y., Kako, T., & Ye, J. (2013). A new heterojunction Ag_3PO_4/Cr-$SrTiO_3$ photocatalyst towards efficient elimination of gaseous organic pollutants under visible light irradiation. Applied Catalysis B: Environmental, 134, 286-292.
17. Han, H., & Bai, R. (2009). Buoyant photocatalyst with greatly enhanced visible-light activity prepared through a low temperature hydrothermal method. Industrial & Engineering Chemistry Research, 48(6), 2891-2898.
18. Han, H., & Bai, R. (2010). Highly effective buoyant photocatalyst prepared with a novel layered-TiO_2 configuration on polypropylene fabric and the degradation performance for methyl orange dye under UV–Vis and Vis lights. Separation and Purification Technology, 73(2), 142-150.
19. Hu, L., Wei, H., Zhang, Y., Zhang, S., & Li, B. (2014). TiO_2/carbon paper composite materials with hierarchically porous structure for photocatalysis. Materials Letters, 119, 88-91.
20. Kondo, Y., Yoshikawa, H., Awaga, K., Murayama, M., Mori, T., Sunada, K., & Iijima, S. (2008). Preparation, photocatalytic activities, and dye-sensitized

solar-cell performance of submicron-scale TiO_2 hollow spheres.Langmuir, 24(2), 547-550.

21. Krýsa, J., Waldner, G., Měšťánková, H., Jirkovský, J., & Grabner, G. (2006). Photocatalytic degradation of model organic pollutants on an immobilized particulate TiO_2 layer: Roles of adsorption processes and mechanistic complexity. Applied Catalysis B: Environmental, 64(3), 290-301.
22. Kwon, C. H., Shin, H., Kim, J. H., Choi, W. S., & Yoon, K. H. (2004). Degradation of methylene blue via photocatalysis of titanium dioxide. Materials Chemistry and Physics, 86(1), 78-82.
23. Lang, X., Chen, X., & Zhao, J. (2014). Heterogeneous visible light photocatalysis for selective organic transformations. Chemical Society Reviews, 43(1), 473-486.
24. Lazar, M. A., Varghese, S., & Nair, S. S. (2012). Photocatalytic water treatment by titanium dioxide: recent updates. Catalysts, 2(4), 572-601.
25. Leong, S., Razmjou, A., Wang, K., Hapgood, K., Zhang, X., & Wang, H. (2014). TiO_2 based photocatalytic membranes: a review. Journal of Membrane Science, 472, 167-184.
26. Lin, H., Ye, H., Xu, B., Cao, J., & Chen, S. (2013). Ag_3PO_4 quantum dot sensitized $BiPO_4$: a novel p–n junction $Ag_3PO_4/BiPO_4$ with enhanced visible-light photocatalytic activity. Catalysis Communications, 37, 55-59.
27. Lin, L., Zhai, S. R., Xiao, Z. Y., Song, Y., An, Q. D., & Song, X. W. (2013). Dye adsorption of mesoporous activated carbons produced from NaOH-pretreated rice husks. Bioresource technology, 136, 437-443.
28. Lin, S. H., Chiou, C. H., Chang, C. K., & Juang, R. S. (2011). Photocatalytic degradation of phenol on different phases of TiO_2 particles in aqueous

suspensions under UV irradiation. Journal of environmental management, 92(12), 3098-3104.

29. Liu, H., Du, C. M., Wang, J., Li, H. X., Zhang, L., & Zhang, L. L. (2012). Comparison of acid Orange 7 degradation in solution by gliding arc discharge with different forms of TiO_2. Plasma Processes and Polymers, 9(3), 285-297.
30. Liu, S., & Chen, X. (2007). Preparation and characterization of a novel activated carbon-supported N-doped visible light response photocatalyst ($TiO_{2-x}Ny$/AC). Journal of Chemical Technology and Biotechnology, 82(5), 453-459.
31. Liu, T. H., Chen, X. J., Dai, Y. Z., Zhou, L. L., Guo, J., & Ai, S. S. (2015). Synthesis of Ag_3PO_4 immobilized with sepiolite and its photocatalytic performance for 2, 4-dichlorophenol degradation under visible light irradiation. Journal of Alloys and Compounds, 649, 244-253.
32. Ma, X., Li, H., Wang, Y., Li, H., Liu, B., Yin, S., & Sato, T. (2014). Substantial change in phenomenon of "self-corrosion" on Ag_3PO_4/TiO_2 compound photocatalyst. Applied Catalysis B: Environmental, 158, 314-320.
33. Nizard, H., Kosinova, M. L., Fainer, N. I., Rumyantsev, Y. M., Ayupov, B. M., & Shubin, Y. V. (2008). Deposition of titanium dioxide from TTIP by plasma enhanced and remote plasma enhanced chemical vapor deposition. Surface and Coatings Technology, 202(17), 4076-4085.
34. Rabbani, M., Bathaee, H., Rahimi, R., & Maleki, A. (2016). Photocatalytic degradation of p-nitrophenol and methylene blue using Zn-TCPP/Ag doped mesoporous TiO_2 under UV and visible light irradiation. Desalination and Water Treatment, 1-9.
35. Rashid, J., & Barakat, M. A. Ag_3PO_4 Enhanced TiO_2 for Visible Light Photocatalysis of 2-Chlorophenol in Wastewater.

36. Rawal, S. B., Do Sung, S., & Lee, W. I. (2012). Novel Ag_3PO_4/TiO_2 composites for efficient decomposition of gaseous 2-propanol under visible-light irradiation. Catalysis Communications, 17, 131-135.
37. Sakthivel, S., Shankar, M. V., Palanichamy, M., Arabindoo, B., & Murugesan, V. (2002). Photocatalytic decomposition of leather dye: comparative study of TiO_2 supported on alumina and glass beads. Journal of Photochemistry and Photobiology A: Chemistry, 148(1), 153-159.
38. Sankapal, B. R., Lux-Steiner, M. C., & Ennaoui, A. (2005). Synthesis and characterization of anatase-TiO_2 thin films. Applied Surface Science,239(2), 165-170.
39. Shan, A. Y., Ghazi, T. I. M., & Rashid, S. A. (2010). Immobilisation of titanium dioxide onto supporting materials in heterogeneous photocatalysis: a review. Applied Catalysis A: General, 389(1), 1-8.
40. Shet, A., & Shetty, V. (2015). Photocatalytic degradation of phenol using Ag core-TiO_2 shell (Ag@ TiO_2) nanoparticles under UV light irradiation.Environmental Science and Pollution Research, 1-10.
41. Shironita, S., Mori, K., Shimizu, T., Ohmichi, T., Mimura, N., & Yamashita, H. (2008). Preparation of nano-sized platinum metal catalyst using photo-assisted deposition method on mesoporous silica including single-site photocatalyst. Applied Surface Science, 254(23), 7604-7607.
42. Singh, S., Chaki, A., Chand, D. P., Raghuwanshi, A., Singh, P. K., & Mahalingham, H. (2014). A novel polystyrene-supported titanium dioxide photocatalyst for degradation of methyl orange and methylene blue dyes under UV irradiation. Journal of Chemical Engineering, 28(1), 9-13.

43. Sriwong, C., Wongnawa, S., & Patarapaiboolchai, O. (2008). Photocatalytic activity of rubber sheet impregnated with TiO_2 particles and its recyclability. Catalysis Communications, 9(2), 213-218.
44. Tennakone, K., Tilakaratne, C. T. K., & Kottegoda, I. R. M. (1995). Photocatalytic degradation of organic contaminants in water with TiO_2 supported on polythene films. Journal of Photochemistry and Photobiology A: Chemistry, 87(2), 177-179.
45. Tong, H., Ouyang, S., Bi, Y., Umezawa, N., Oshikiri, M., & Ye, J. (2012). Nano-photocatalytic materials: possibilities and challenges. Advanced materials, 24(2), 229-251.
46. Wan, J., Sun, L., Fan, J., Liu, E., Hu, X., Tang, C., & Yin, Y. (2015). Facile synthesis of porous Ag_3PO_4 nanotubes for enhanced photocatalytic activity under visible light. Applied Surface Science, 355, 615-622.
47. Wang, H., Bai, Y., Yang, J., Lang, X., Li, J., & Guo, L. (2012). A facile way to rejuvenate Ag_3PO_4 as a recyclable highly efficient photocatalyst.Chemistry–A European Journal, 18(18), 5524-5529.
48. Xu, Y. S., & Zhang, W. D. (2013). Monodispersed Ag_3PO_4 nanocrystals loaded on the surface of spherical $Bi_2M_oO_6$ with enhanced photocatalytic performance. Dalton Transactions, 42(4), 1094-1101.
49. Yang, J. H., Han, Y. S., & Choy, J. H. (2006). TiO_2 thin-films on polymer substrates and their photocatalytic activity. Thin Solid Films, 495(1), 266-271.
50. Yi, Z., Ye, J., Kikugawa, N., Kako, T., Ouyang, S., Stuart-Williams, H., & Liu, Y. (2010). An orthophosphate semiconductor with photooxidation properties under visible-light irradiation. Nature Materials, 9(7), 559-564.

51. Yi, Z., Ye, J., Kikugawa, N., Kako, T., Ouyang, S., Stuart-Williams, H., ... & Liu, Y. (2010). An orthophosphate semiconductor with photooxidation properties under visible-light irradiation. Nature Materials, 9(7), 559-564.
52. Yuranova, T., Enea, O., Mielczarski, E., Mielczarski, J., Albers, P., & Kiwi, J. (2004). Fenton immobilized photo-assisted catalysis through a Fe/C structured fabric. Applied Catalysis B: Environmental, 49(1), 39-50.
53. Yuranova, T., Mosteo, R., Bandara, J., Laub, D., & Kiwi, J. (2006). Self-cleaning cotton textiles surfaces modified by photoactive SiO_2/TiO_2 coating. Journal of Molecular Catalysis A: Chemical, 244(1), 160-167.
54. Zhang, L., Zhang, H., Huang, H., Liu, Y., & Kang, Z. (2012). Ag_3PO_4/SnO_2 semiconductor nano-composites with enhanced photocatalytic activity and stability. New Journal of Chemistry, 36(8), 1541-1544.
55. Zhang, M., Wu, J., Lu, D., & Yang, J. (2013). Enhanced visible light photocatalytic activity for TiO_2 nanotube array films by codoping with tungsten and nitrogen. International Journal of Photoenergy, 2013.
56. Zhao, F. M., Pan, L., Wang, S., Deng, Q., Zou, J. J., Wang, L., & Zhang, X. (2014). Ag_3PO_4/TiO_2 composite for efficient photodegradation of organic pollutants under visible light. Applied Surface Science, 317, 833-838.
57. Zhiyong, Y., Keppner, H., Laub, D., Mielczarski, E., Mielczarski, J., Kiwi-Minsker, L., ... & Kiwi, J. (2008). Photocatalytic discoloration of Methyl Orange on innovative parylene–TiO_2 flexible thin films under simulated sunlight. Applied Catalysis B: Environmental, 79(1), 63-71.
58. Zhiyong, Y., Laub, D., Bensimon, M., & Kiwi, J. (2008). Flexible polymer TiO_2 modified film photocatalysts active in the photodegradation of azo-dyes in solution. Inorganica Chimica Acta, 361(3), 589-594.